THIRD TSUNAMI SYMPOSIUM PAPERS

OBJECTIVE: **The Tsunami Society** publishes this journal to increase and disseminate knowledge about tsunamis and their hazards.

DISCLAIMER: Although these articles have been technically reviewed by peers, **The Tsunami Society** is not responsible for the veracity of any statement, opinion or consequences.

Submit manuscripts of articles, notes or letters to the Editor. If an article is accepted for publication the author(s) must submit a scan ready manuscript, a TeX or a PDF file in the journal format. Issues of the journal are published electronically in PDF format. Recent journal issues are available at
http://www.sthjournal.org.

Tsunami Society members will be advised by e-mail when a new issue is available. There are no page charges or reprints for authors.

Permission to use figures, tables and brief excerpts from this journal in scientific and educational works is hereby granted provided that the source is acknowledged.

Issues of the journal from 1982 thru 2005 are available in PDF format at
http://epubs.lanl.gov/tsunami/
and on a CD-ROM from the Society to Tsunami Society members.

NUMERICAL MODEL FOR THE KRAKATOA HYDROVOLCANIC EXPLOSION AND TSUNAMI

Charles L. Mader
Mader Consulting Co.
Honolulu, HI 96825 U.S.A.

Michael L. Gittings
Science Applications International Corporation
Los Alamos, NM 87544 U.S.A.

ABSTRACT

Krakatoa exploded August 27, 1883 obliterating 5 square miles of land and leaving a crater 3.5 miles across and 200-300 meters deep. Thirty three feet high tsunami waves hit Anjer and Merak demolishing the towns and killing over 10,000 people. In Merak the wave rose to 135 feet above sea level and moved 100 ton coral blocks up on the shore.

Tsunami waves swept over 300 coastal towns and villages killing 40,000 people. The sea withdrew at Bombay, India and killed one person in Sri Lanka.

The tsunami was produced by a hydrovolcanic explosion and the associated shock wave and pyroclastic flows.

A hydrovolcanic explosion is generated by the interaction of hot magma with ground water. It is called Surtseyan after the 1963 explosive eruption off Iceland. The water flashes to steam and expands explosively. Liquid water becoming water gas at constant volume generates a pressure of 30,000 atmospheres.

The Krakatoa hydrovolcanic explosion was modeled using the full Navier-Stokes AMR Eulerian compressible hydrodynamic code called SAGE which includes the high pressure physics of explosions.

The water in the hydrovolcanic explosion was described as liquid water heated by the magma to 1100 degree Kelvin or 19 kcal/mole. The high temperature water is an explosive with the hot liquid water going to a water gas. The BKW steady state detonation state has a peak pressure of 89 kilobars, a propagation velocity of 5900 meters/second and the water is compressed to 1.33 grams/cc.

The observed Krakatoa tsunami had a period of less than 5 minutes and wavelength of less than 7 kilometers and thus rapidly decayed. The far field tsunami wave was negligible. The air shock generated by the hydrovolcanic explosion propagated around the world and coupled to the ocean resulting in the explosion being recorded on tide gauges around the world.

INTRODUCTION

The Krakatoa volcanic explosion and its consequences are described in detail by George Pararas-Carayannis in reference 1 and Simon Winchester in reference 2.

Krakatoa exploded August 27, 1883 obliterating 5 square miles of land and leaving a crater 3.5 miles across and 200-300 meters deep. Thirty three feet high tsunami waves hit Anjer and Merak, demolishing the towns and killing over 10,000 people. In Merak the wave rose to 135 feet above sea level and moved 100 ton coral blocks up on the shore. Tsunami waves swept over 300 coastal towns and villages killing 40,000 people. The sea withdrew at Bombay, India and killed one person in Sri Lanka.

The tsunami was produced by a hydrovolcanic explosion and the associated shock wave and pyroclastic flows.

A hydrovolcanic explosion is generated by the interaction of hot magma with ground water. It is called Surtseyan after the 1963 explosive eruption off Iceland. The water flashes to steam and expands explosively. Liquid water becoming water gas at constant volume generates a pressure of 30,000 atmospheres.

The Krakatoa hydrovolcanic explosion was modeled using the full Navier-Stokes AMR Eulerian compressible hydrodynamic code called SAGE with includes the high pressure physics of explosions.

The observed Krakatoa tsunami had a period of less than 5 minutes and wavelength of less than 7 kilometers and thus rapidly decayed. The far field tsunami wave was negligible. The air shock generated by the hydrovolcanic explosion propagated around the world and coupled to the ocean resulting in the explosion being recorded on tide gauges around the world.

NUMERICAL MODELING

The compressible Navier-Stokes equations are described in reference 3 and 4 and examples of many numerical solutions of complicated physical problems are described. The compressible Navier-Stokes equations are solved by a high-resolution Godunov differencing scheme using an adaptive grid technique described in reference 5.

The solution technique uses Continuous Adaptive Mesh Refinement (CAMR). The decision to refine the grid is made cell-by-cell continuously throughout the calculation. The computing is concentrated on the regions of the problem which require high resolution.

Refinement occurs when gradients in physical properties (density, pressure, temperature, material constitution) exceed defined limits, down to a specified minimum cell size for each material. The mesh refinement is described in detail in reference 3.

Much larger computational volumes, times and differences in scale can be simulated than possible using previous Eulerian techniques such as those described in reference 4.

The original code was called SAGE. A later version with radiation is called RAGE. A recent version with the techniques for modeling reactive flow described in reference 3 is called NOBEL. It was used for the modeling of hydrovolcanic explosions described in this paper.

Some of the remarkable advances in fluid physics using the SAGE code have been the modeling of Richtmyer-Meshkov and shock induced instabilities described in references

6 and 7. It was used for modeling the Lituya Bay impact landslide generated tsunami and water cavity generation described in references 8 and 9. NOBEL/SAGE/RAGE were used to model the generation of water cavities by projectiles and explosions and the resulting water waves in reference 10. The codes were used to model asteroid impacts with the ocean and the resulting tsunami waves in references 11 and 12.

The codes can describe one-dimensional slab or spherical geometry, two-dimensional slab or cylindrical geometry, and three-dimensional Cartesian geometry.

Because modern supercomputing is currently done on clusters of machines containing many identical processors, the parallel implementation of the code is very important. For portability and scalability, the codes use the Message Passing Interface (MPI). Load leveling is accomplished through the use of an adaptive cell pointer list, in which newly created daughter cells are placed immediately after the mother cells. Cells are redistributed among processors at every time step, while keeping mothers and daughters together. If there are a total of M cells and N processors, this technique gives nearly (M / N) cells per processor. As neighbor cell variables are needed, the MPI gather/scatter routines copy those neighbor variables into local scratch memory.

The calculations described in this paper were performed on IBM NetVista and ThinkPad computers and did not require massive parallel computers.

The codes incorporate multiple material equations of state (analytical or SESAME tabular). Every cell can in principle contain a mixture of all the materials in a problem assuming that they are in pressure and temperature equilibrium.

As described in reference 4, pressure and temperature equilibrium is appropriate only for materials mixed molecularly. The assumption of temperature equilibrium is inappropriate for mixed cells with interfaces between different materials. The errors increase with increasing density differences. While the mixture equations of state described in reference 4 would be more realistic, the problem is minimized by using fine numerical resolution at interfaces. The amount of mass in mixed cells is kept small resulting in small errors being introduced by the temperature equilibrium assumption.

Very important for hydrovolcanic explosions, water cavity collapse and the resulting water wave history is the capability to initialize gravity properly, which is included in the code. This results in the initial density and initial pressure changing going from the atmosphere at 2 kilometers altitude down to the ocean surface.   Likewise the water density and pressure changes correctly with ocean depth.

HYDROVOLCANIC MODEL

A hydrovolcanic explosion is generated by the interaction of hot magma with ground water. It is called Surtseyan after the 1963 explosive eruption off Iceland. The water flashes to steam and expands explosively. Liquid water becoming water gas at constant volume generates a pressure of 30,000 atmospheres.

The Krakatoa hydrovolcanic explosion was modeled using the full Navier-Stokes AMR Eulerian compressible hydrodynamic code called SAGE with includes the high pressure physics of explosions.

The water in the hydrovolcanic explosion was described as liquid water heated by the magma to 1100 degree Kelvin or 19 kcal/mole. The high temperature water is an explosive with the hot liquid water going to a water gas. The BKW steady state detonation state described in reference 4 has a peak pressure of 89 kilobars, a propagation velocity of 5900 meters/second and the water is compressed to 1.33 grams/cc.

THE KRAKATOA MODEL

 The island of Krakatoa today and before 1883 are shown in Figure 1.
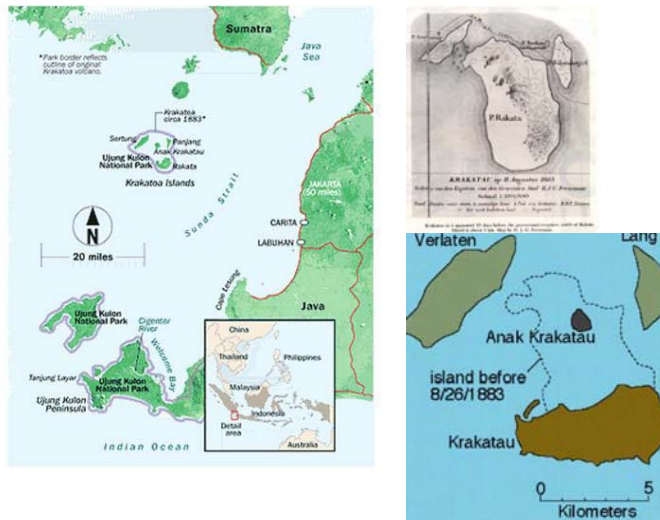
Figure 1. Maps of Krakatoa today and before 1883.

  It was modeled in two-dimensions as a spherical island 200 meters high above the ocean level and 3 kilometers in radius tapering down to ocean level by 4 kilometers as shown in Figure 2. The ocean was 100 meters deep and extended in the rock under the island. The lava was initially assumed to interact with the water in the center of the island in a 500 meter radius hot spot region. The propagating hydrovolcanic explosion propagated outward at about 5900 meters per second and at a constant volume pressue of about 30,000 atmospheres as shown in Figure 3.
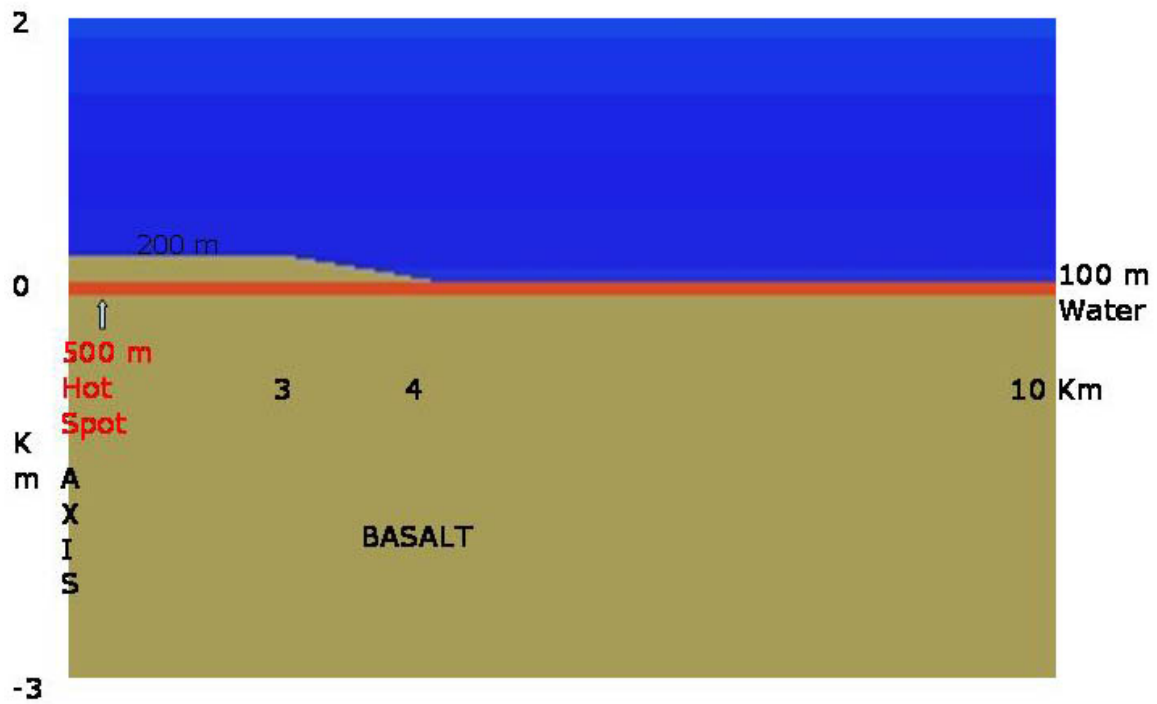
Figure 2. The spherical model for the Krakatoa hydrovolcanic explosion.
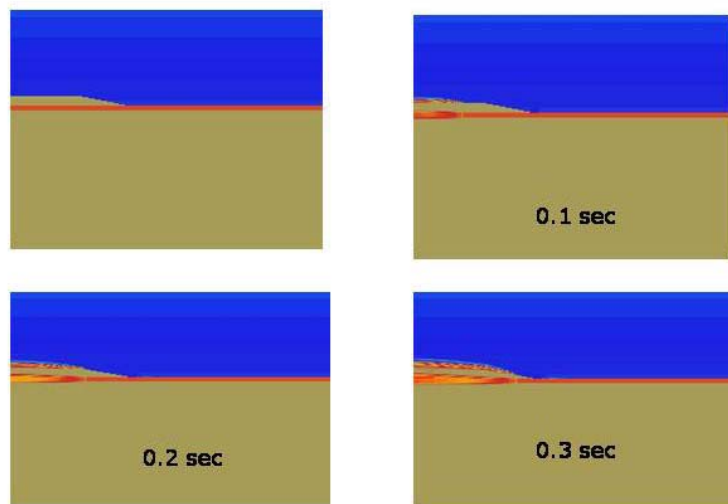
Figure 3. The propagating hydrovolcanic explosion.

The expansion of the hydrovolcanic explosion is shown in Figures 4 and 5 at various times up to 10 seconds as density picture plots.
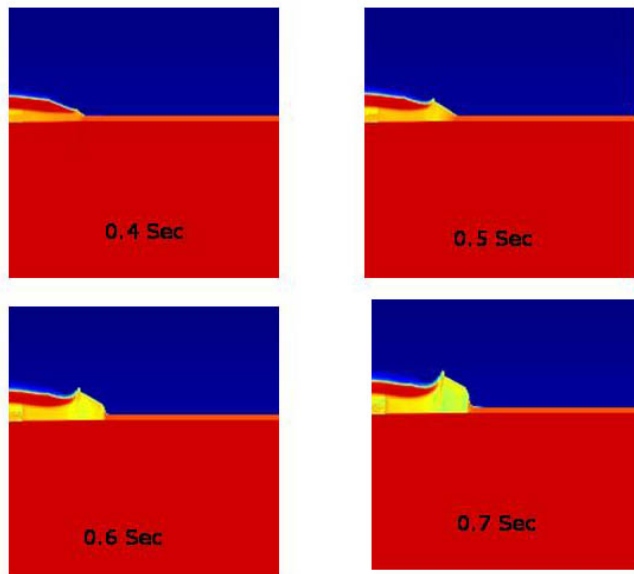
Figure 4.   The density profile at various times for the hydrovolcanic explosion of Krakatoa.
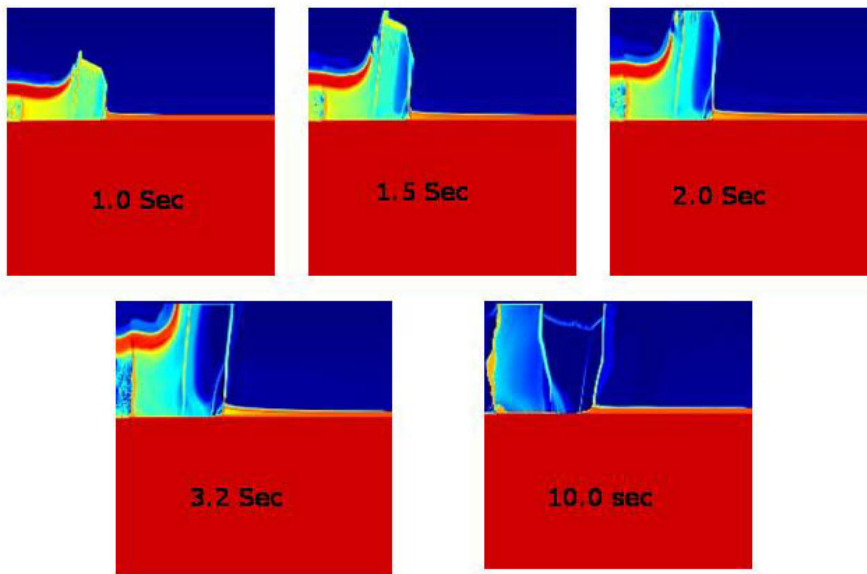
Figure 5. The density profile at later times for the hydrovolcanic explosion of Krakatoa.

The velocity contour picture plots in the X-direction are shown in Figure 6.   The propagation of the shock wave in the basalt below the island, the basalt above sea level, the water and in the air is shown.
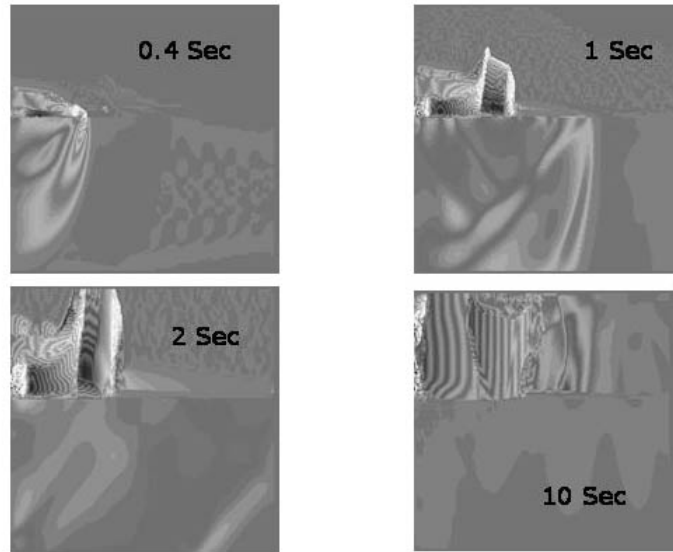
Figure 6. The velocity profiles in the horizontal or X-Direction at various times.

The water wave profiles at 4, 5, and 8 kilometers are shown in Figure 7. The wave outside the hydrovolcanic explosion at 4 km is 130 meters high and decays to 48 meters by 5 kilometers and to 7.5 meters at 8 kilometers.
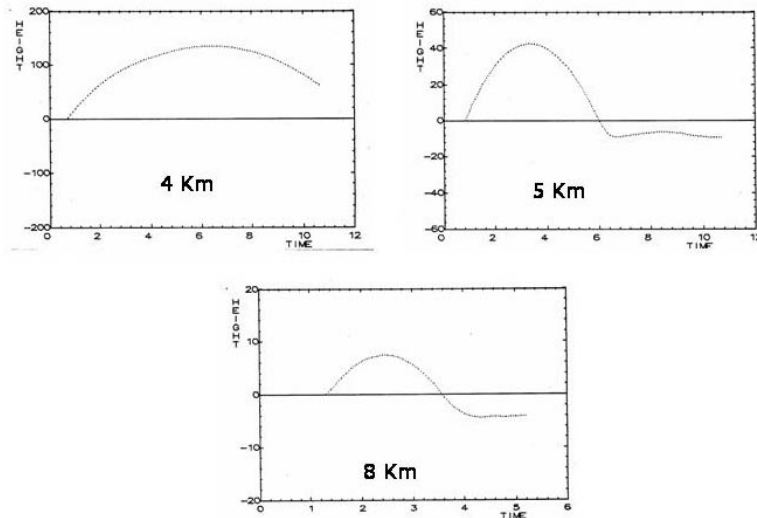
Figure 7. The water wave profiles as a function of time at 4, 5 and 8 km.

The states of the water at 1.5 kilometers in the middle of the hydrovolcanic explosion of the water reached pressures greater than 25,000 bars and expanded to altitudes greater than 2 kilometers and drove the Krakatoa island basalt to altitudes greater than 2 kilometers. Perhaps the hydrovolcanic explosion looked something like 1946 Bikini nuclear explosion shown in Figure 8 without the warships. The Baker shot was a 21 kiloton device fired at 27 meter depth in the ocean. The Krakatoa event released 150-200 megatons.

Figure 8. The 1946 Bikini Atomic Explosion.

CONCLUSIONS

A fully-compressible reactive hydrodynamic model for the process of hydrovolcanic explosion of liquid water to steam at constant volume and pressures of 30,000 atmospheres has been applied to the explosion of Krakatoa in 1883. The idealized spherical geometry exhibits the general characteristics observed including the destruction of the island and the projection of the island into high velocity projectiles that travel into the high upper atmosphere above 2 kilometers. A high wall of water is formed that is initially higher than 100 meters driven by the shocked water, basalt and air. The initial wave period of about 30 seconds and the rapid decay of the water wave suggests that the hydrovolcanic explosion in the calculation was less than in the Krakatoa explosion. The idealized 2-D geometry needs to be replaced with a realistic 3-D one. The hydrovolcanic process needs to involve a more accurate description of the water filled porous basalt layer where the hydrovolcanic explosion occurs.

REFERENCES

1. George Pararas-Carayannis, "Near and Far-Field Effects of Tsunamis Generated by the Paroxysmal Eruptions, Explosions, Caldera Collapses and Massive Slope Failures of the Krakatau Volcano in Indonesia on August 26-27, 1883," Science of Tsunami Hazards, Vol. 21, No. 4, pp 191-2l1 (2003).

2. Simon Winchester, **Krakatoa**, Harper Collins Publishers, New York, NY (2003)

3. Charles L. Mader, **Numerical Modeling of Water Waves- Second Edition**, CRC Press, Boca Raton, Florida (2004).

4. Charles L. Mader, **Numerical Modeling of Explosives and Propellants**, CRC Press, Boca Raton, Florida (1998).

5. M. L. Gittings, "1992 SAIC's Adaptive Grid Eulerian Code," Defense Nuclear Agency Numerical Methods Symposium, pp. 28-30 (1992).

6. R. L. Holmes, G. Dimonte, B. Fryxell, M. L. Gittings, J. W. Grove, M. Schneider, D. H. Sharp, A. L. Velikovich, R. P. Weaver and Q. Zhang, "Richtmyer-Meshkov Instability Growth: Experiment, Simulation and Theory," Journal of Fluid Mechanics, Vol. 9, pp. 55-79 (1999).

7. R. M. Baltrusaitis, M. L. Gittings, R. P. Weaver, R. F. Benjamin and J. M. Budzinski, "Simulation of Shock-Generated Instabilities," Physics of Fluids, Vol. 8, pp. 2471-2483 (1996).

8. Charles L. Mader, "Modeling the 1958 Lituya Bay Tsunami," Science of Tsunami Hazards, Vol. 17, pp. 57-67 (1999).

9. Charles L. Mader, "Modeling the 1958 Lituya Bay Mega-Tsunami, II ," Science of Tsunami Hazards, Vol. 20, pp. 241-250 (2002).

10. Charles L. Mader and Michael L. Gittings, "Dynamics of Water Cavity Generation," Science of Tsunami Hazards, Vol. 21, pp. 91-118 (2003).

11. Galen Gisler, Robert Weaver, Michael L. Gittings and Charles Mader, "Two- and Three-Dimensional Simulations of Asteroid Ocean Impacts," Science of Tsunami Hazards, Vol. 21, pp. 119-134 (2003).

12. Galen Gisler, Robert Weaver, Michael L. Gittings and Charles Mader, "Two- and Three-Dimensional Asteroid Impact Simulations," Computers in Science and Engineering (2004).

PERSISTENT HIGH WATER LEVELS AROUND ANDAMAN & NICOBAR ISLANDS FOLLOWING THE 26 DECEMBER 2004 TSUNAMI

N. Nirupama
School of Administrative Studies
York University
Toronto, Canada
T.S. Murty and I. Nistor
Department of Civil Engineering
University of Ottawa
Ottawa, Canada
A.D. Rao
Centre for Atmospheric Sciences
Indian Institute of Technology
New Delhi, India

ABSTRACT

During the tsunami of 26th December 2004 in the Indian Ocean, media reports suggested that high water levels persisted around the Andaman & Nicobar Islands for several days. These persistent high water levels can be explained by invoking the existence of trapped and partially leaky modes on the shelves surrounding these islands. It has been known in the studies of tides in the global oceans, that there are two distinct types of oscillations, separated in their frequencies by the period of the pendulum day. One species are the gravity waves, and the others are the rotational waves, associated with earth's rotation. Both these species can be found in tidal records around islands as well as near coastlines. Essentially these are either trapped or partly leaky modes, partly trapped on the continental shelves. These two types of modes are usually found in the tsunami records on tide gauges. The tide gauge records as well as visual descriptions of the water levels during and after the occurrence of a tsunami clearly show the presence of these oscillations.

1.   INTRODUCTION

The analysis of tidal observations revealed that there are two distinct types of oscillations in the oceans that are separated in their frequencies through the pendulum day. One species are the gravity waves, also referred to as Gravoids modes or Oscillations of the First Class (OFC). The second species are Oscillations of the Second Class (OSC) or rotational modes and are also called Elastoid-inertia oscillations. The first class has gravity explicitly in their frequency equation, while for the second class, which owe their existence to earth's rotation, gravity does not play an important role in their frequencies.   The importance of these two types of oscillations in the world oceans is known for a long time, and especially in the tide gauge records near coastlines with wide continental shelves and also in tidal records around islands. The bathymetry of the wide shelf near a coastline or the bathymetry on the shelf surrounding an island can trap a significant amount of long gravity energy associated with such events as tsunamis and storm surges and retain it on the shelf for several days, if not weeks, until the trapped energy slowly leaks away out of the shelf.

The so-called trapped and leaky modes are really the OFC and OSC and can be deduced by analyzing the tide gauge records of tsunamis and storm surges. Specifically in this study we examined the situation of persistent high water levels around the Andaman & Nicobar Islands located in the Bay of Bengal, for the tsunami of 26th December 2004 in the Indian Ocean (Figure 1). Figure 2 shows a detailed map of the Andaman & Nicobar Islands region. Media reports suggested that high water levels persisted around these islands for several days even after the tsunami, and we suggest trapped modes as the most probable cause.

Here we present some theory and some simple analytical calculation which shows that oscillations with periods of few minutes are possible. Observations seem to suggest that most probably this was the case. However, an exact comparison has to wait until we complete a more sophisticated numerical model study is completed as well as a thorough analysis of all the available tide gauge records. But one result that has become obvious even in this preliminary study is that in the trapped modes around Andaman & Nicobar Islands following the tsunami, there were several oscillations with periods of the order of several minutes, and we suggest that these are the Gravoid and Elastoid modes.

Figure 1: Northern part of the Indian Ocean (Courtesy of the University of Texas Libraries, The University of Texas at Austin)
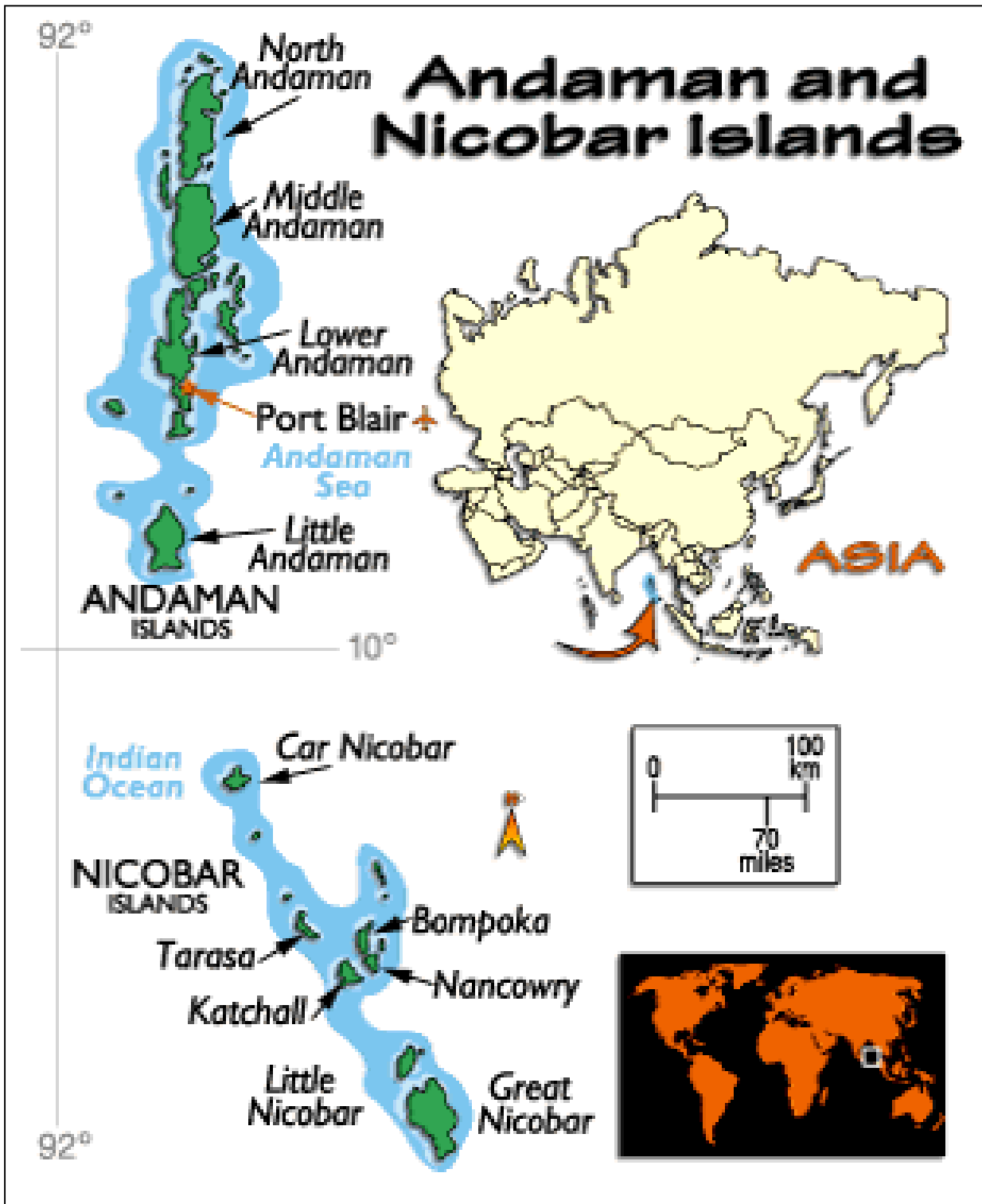
Figure 2: Detailed map of Andaman & Nicobar Islands (www.andamanconnections.com)

2.   Oscillations of the first class (OFC) and the second class (OSC)

Laplace (quoted by Lamb, 1932) classified the tidal phenomenon into zonal and tesseral oscillations. In the zonal oscillation, the surface of the liquid is divided into annular zones symmetric with respect to the vertical axis through some hypothetical geometric center. In the tesseral oscillations, the surface of the liquid is divided into a number of compartments, by nodal circles and nodal diameters.

In the tesseral oscillations, Hough (1898) distinguished between OFC (Oscillations of the First Class) and OSC (Oscillations of the Second Class) in the following manner. If σ is the frequency of oscillation, and ω the frequency of rotation, then OFC are those for which:

$$\sigma = \sigma_0 \ (\neq 0)$$
$$\text{As } \omega \rightarrow 0 \tag{1}$$

And OSC are those for which

$$\sigma \rightarrow O \ (\omega)$$
$$\text{As } \omega \rightarrow 0 \tag{2}$$

Bjerknes et al. (1934) distinguished between OFC and OSC through the dimensionless ratio $\sigma/2\omega$ as follows:

$$\frac{\sigma}{2\omega} \begin{cases} \geq 1.........GravityModes(OFC) \\ \leq 1.........Elastoid - InertiaModes(OSC) \end{cases} \tag{3}$$

As $\dfrac{\sigma}{2\omega}$ approaches unity from higher values, gravity modes tend to disappear. For the gravity modes, gravity appears explicitly in the frequency equation. For the rotational modes (Elastoid-inertia oscillations), the frequency for a given mode is a function, mainly of the ratio of the depth of the liquid, to the radius of the container (assumed to be an idealized circular waterbody) and gravity does not play an important role in the frequency equation.

While the intertial stability associated with rotation is a necessary condition for the existence of OSC, it is not a necessary condition for the existence of OFC. Hence, one can ask the question, what is the effect of earth's rotation on gravity waves, such as tides, tsunamis and storm surges, specifically on their frequencies, besides the well recognized effect of the Coriolis force? Kelvin (1879) partly answered this question in his studies on tidal motions on a rotating earth. He gave the following simple relation:

$$\sigma^2 = \sigma_0^2 + 4\omega^2 \tag{4}$$

Where, ω = Rotation frequency
σ_0 = Frequency of the gravity mode without the influence of earth's rotation
σ = Frequency of the gravity mode when the influence of earth's rotation is included

Eq. (4) is valid when the ellipticity associated with earth's rotation is ignored, in other words, for Eq. (4) to be valid, earth's rotation should have no influence on the free surface of the ocean, i.e. the free surface is always flat, which of course is not the case. However, Eq. (4) is still valid at least in a qualitative sense. It shows that rotation increases the frequency and thus increases the restoring tendency of the system (if the system is perturbed by some external force). However, if the ellipticity is included, this may not always be the case, especially for the higher modes (Murty, 1962).

3. Trapped and Partially Leaky Modes

The trapped and leaky modes concept can be formulated in terms of the OFC and OSC explained in Section 2 (Murty et al., 2005). Eckart (1950) recognized that gravity waves generated in shallow water might get totally reflected while proceeding into deep water at the continental slope. Isacks et al. (1951) used ray theory concepts to show that these waves could be captured from the open sea and guided along a long coastline by successive reflections between the shoreline and the offshore water. Snodgrass et al. (1962) showed from theory that trapped waves could exist along California's borderland, and from spectral analysis of long-wave records they pointed out that the shoreline is a good reflector for long-wave energy. Munk et al. (1964) made observations especially designed to isolate the trapped waves from other motions and concluded that trapped waves account for most low-frequency energy. The important fact that tsunamis approaching a coast can generate trapped waves has been conclusively shown with reference to the Japanese coast by Hatori and Takahasi (1964), Aida (1967), and Hatori (1967). Summerfield (1969) pointed out some unclear use of the terms "trapped waves" and "edge waves".

Stokes (1846), the first to discover these theoretically, used the linearized forms of the surface-wave equations. Ursell (1952) not only found higher-order edge waves but demonstrated their existence in laboratory experiments. Trapping gravity wave energy (caused by guiding waves along the continental shelf) is somewhat analogous to other wave guides in geophysical problems (e.g. Love waves in the earth's crust and sound waves in the Sound Fixing and Ranging (SOFAR) channel in the oceans). An important paper on trapped modes is Longuet-Higgins (1967) who showed that isolated islands might trap long waves that are guided by local bathymetry. The observation that prompted Longuet-Higgins work is the long-wave records at Macquarie Island (54°34′S, 158°58′E) which clearly showed an oscillation period of 6 min and a beat period of 3 h.

The so-called oscillations of the second class (OSC) owe their existence to the earth's rotation. These waves also could get trapped like the gravity waves discussed earlier.

Reid (1958), while studying the effect of Coriolis force on OFC, found another type of very low-frequency motions that propagate along (in the same direction as Kevin waves) and are almost confined to the shoreline, which he called quasi-geostrophic boundary waves. For these waves, the longshore component of the fluid flow and the offshore wave slope approximately balance each other.

Two extreme cases arise: the longshore wavelength of these waves is much less or much greater than the width of the shelf. In the former case, Mysak (1968) showed that the finite width of the shelf has no influence on the waves whereas in the latter case, Robinson (1964) showed that the waves are more or less confined to shallow water and he named these free, second-class, surface wave motions "continental shelf waves."

The motions considered here under OSC have periods greater than a pendulum day, defined as the period of revolution of a Foucault's pendulum. This is given by:

$$\text{Pendulum day} = 2T_p = \frac{2\pi}{\Omega \cdot \sin\theta} \tag{5}$$

Where θ is the latitude and Ω is the angular velocity of earth's rotation. This expression shows that the pendulum day varies from place to place, depending on latitude. It is $2\pi/\Omega$ at the pole and tends to ∞ at the equator. When the rotation $\Omega \to 0$ the OSC become steady currents. Crease (1956) speculated that in a uniformly rotating ocean of uniform depth the existence of a trapped long wave along a finite length straight-line barrier is possible. The works of Chambers (1964) and Williams (1964) verified Crease's suggestion. A similar phenomenon was discovered by Sekerzh-Zen'kovich (1968) for a cylindrical island in an ocean of uniform depth. These special types of OSC propagate along the barrier or island in the same sense as a Kelvin wave. However, although the motions exist only in the presence of rotation, they have periods less than a pendulum day and in that sense do not belong strictly to OSC.

4.   Computation of the Periods of Trapped Modes

Yanuma and Tsuji (1998) gave the following relationship for edge wave modes trapped on the continental shelf:

$$\omega^2 = \frac{(2N+1)(2M+1) \cdot \pi \cdot \alpha \cdot g}{2L} \tag{6}$$

Where, α = slope of the shelf
ω = angular frequency of the edge wave mode
g = acceleration due to gravity = 9.8 m/sec^2
L = width of the shelf
N = number of the progressive edge wave mode
M = number of the standing edge wave mode

Period of the edge wave mode = $T = 2\pi/\omega$ (7)

For standing edge wave modes, N = 0
The period of standing edge wave modes is given by:

$$T = \frac{2\pi\sqrt{2L}}{\sqrt{(2M+1)\cdot\pi\cdot\alpha\cdot g}}$$ (8)

If we take L = 1 km and α = 1/1000, for the first standing edge wave mode, M = 0

$$T_{S_0} = \frac{2\pi\sqrt{2\times1000}}{\dfrac{3.14\times9.8}{1000}} \text{ seconds} = \frac{2\sqrt{2}\times3.14\times1000}{\sqrt{3.14\times9.8}\times60} \text{ minutes} = 26.7 \text{ minutes}$$

Table 1 lists the periods for $T_{S_0}, T_{S_1}, T_{S_2}, T_{S_3}$ for different values of shelf width L and shelf slope, α.

Table 1: Periods of the trapped standing edge wave modes for different shelf widths and slopes

Shelf Width L (km)	Shelf Slope α	Modal Number M	Period (Minutes)	Shelf Width L (km)	Shelf Slope α	Modal Number M	Period (Minutes)
1	1/1000	0	26.7	10	1/1000	0	84.38
1	1/1000	1	15.41	10	1/1000	1	48.72
1	1/1000	2	11.93	10	1/1000	2	37.74
1	1/1000	3	10.09	10	1/1000	3	31.89
1	1/100	0	8.44	10	1/100	0	26.68
1	1/100	1	4.87	10	1/100	1	15.41
1	1/100	2	3.77	10	1/100	2	11.93
1	1/100	3	3.19	10	1/100	3	10.09
1	1/10	0	2.67	10	1/10	0	8.44
1	1/10	1	1.54	10	1/10	1	4.87
1	1/10	2	1.19	10	1/10	2	3.77
1	1/10	3	1.01	10	1/10	3	3.19
2	1/1000	0	37.74	20	1/1000	0	119.33
2	1/1000	1	21.79	20	1/1000	1	68.90
2	1/1000	2	16.88	20	1/1000	2	53.37
2	1/1000	3	14.26	20	1/1000	3	45.10
2	1/100	0	11.93	20	1/100	0	37.74
2	1/100	1	6.89	20	1/100	1	21.79
2	1/100	2	5.34	20	1/100	2	16.88
2	1/100	3	4.51	20	1/100	3	14.26
2	1/10	0	3.77	20	1/10	0	11.93

2	1/10	1	2.18	20	1/10	1	6.89
2	1/10	2	1.69	20	1/10	2	5.34
2	1/10	3	1.43	20	1/10	3	4.51
5	1/1000	0	59.67	50	1/1000	0	188.68
5	1/1000	1	34.45	50	1/1000	1	108.94
5	1/1000	2	26.68	50	1/1000	2	84.38
5	1/1000	3	22.55	50	1/1000	3	71.32
5	1/100	0	18.87	50	1/100	0	59.67
5	1/100	1	10.89	50	1/100	1	34.45
5	1/100	2	8.44	50	1/100	2	26.68
5	1/100	3	7.13	50	1/100	3	22.55
5	1/10	0	5.97	50	1/10	0	18.87
5	1/10	1	3.44	50	1/10	1	10.89
5	1/10	2	2.67	50	1/10	2	8.44
5	1/10	3	2.26	50	1/10	3	7.13

For the partially leaky modes, the progressive wave number N will be an integer higher than zero. Table 1 listed the periods for the case N = 0. For the Mode N = 1, the periods can be obtained by dividing the corresponding value in Table 1 by $\sqrt{3}$ or 1.732. For the mode with N = 2, the periods can be obtained by dividing the corresponding value in Table 1 by $\sqrt{5}$ or 2.236. Similar procedure can be used for the higher modes.

CONCLUSIONS

Some theoretical arguments and some simple analytical computations are presented here to explain that the reason for persistent high water levels around the Andaman & Nicobar Islands following the tsunami of 26th December 2004 in the Indian Ocean is the presence of the so-called Gravoid and Elastoid modes of oscillation. These modes are oscillations due to trapping of the long gravity wave energy associated with the tsunami, on the shelf surrounding these islands. While the results presented here are mostly based on theory and some simple analytical calculations, the study is now being expanded to do a proper numerical model as well as analyze all the available tide gauge records. While an exact comparison cannot be made until the numerical model computations are completed, it is worthwhile noting that, the periods of oscillations, of the order of several minutes, in the persistent high water levels around Andaman & Nicobar Islands following the tsunami, that were reported in the media, do agree reasonably well with the results of the simple calculation presented here.

REFERENCES

Aida, I. (1967). Water Level Oscillations on the Continental Shelf in the Vicinity of Miyagy-Enoshima. Bull. Earthquake Res. Inst. 45: 61-78.

Chambers, L. G. (1964). Long Waves on a Rotating Earth in the Presence of a Semi-Infinite barrier. Proc. Edinburgh Math. Soc. 14: 25-31.

Crease, J. (1956). Long Waves on a Rotating Earth in the Presence of a Semi-Infinite barrier. J. Fluid Mech. 1: 86-96.

Eckart, C. (1950). The Ray-Particle Analogy. J. Mar. Res. 9: 139-144.

Hatori, T. (1967). The Wave Form of Tsunami on the Continental Self. Bull. Earthquake Res. Inst. 45: 79-90.

Hatori, T., and R. Takahasi. (1964). On the Iturup Tsunami of Oct. 13, 1963 as Observed Along the Coast of Japan. Bull. Earthquake Res. Inst. 42: 543-554.

Hough, S.S. (1898). On the Application of Hapmonic Analysis to the Dynamical Theory of the Tides. Part II. On the General Integration of Laplace's Dynamical Equations, Phil. Trans. Roy. Soc. London, Ser A, Vol. 191, pp. 138-185

Isacks, J. D., E. A. Williams, and C. Eckart. (1951). Total Reflection of Surface Waves by Deep Water. Trans. Am. Geophys. Union 32: 37-40.

Kelvin. Lord. (1879). On Gravitational Oscillations of Rotating Water, Proc. Roy. Soc. Edinburgh, Vol. 10 (pp. 92-109), Papers, Vol. 4, pp. 141-148

Lamb, H. (1932). Hydrodynamics, 6th Edition, Dover Publishers, New York.

Longuet-Higgins, M.S. (1967). On the Wave-Induced Difference in the Mean Sea Level Between the Two Sides of a Submerged Breakwater. J. Mar. Res. 25: 148-153.

Munk, W. H., F. E. Snodgrass, and F. Gilbert. (1964). Edge Waves on the Continental Shelf: An Experiment to Separate Trapped and Leaky Modes. J. Fluid Mech. 20: 529-554.

Murty, T.S. (1962). Gravity Modes in a Rotating Paraboloidal Dish, M.S. Thesis, Department of Meteorology, University of Chicago, USA, 84 pages.

Murty, T.S., N. Nirupama, A.D. Rao and I. Nistor (2005). Role of Trapped and Leaky Modes around Andaman & Nicobar Islands: Tsunami of 26 December 2004, Workshop on Tsunami Effects and Mitigation Measures, IIT Madras, India, 26 December, 3-21.

Mysak, L. A. (1968a). Edge Waves on a Gently Sloping Continental Shelf of Finite Width. J. Mar. Res. 26: 24-33.

Reid, R. O. (1958) Effects of Coriolis Force on Edge Waves. Part I. Investigations of the Normal Modes. J. Mar. Res. 16: 109-144.

Robinson, A. R. (1964). Continental Shelf Waves and the Response of Sea Level to Weather Systems. J. Geophys. Res. 69: 367-368.

Sekerzh-Zen'Kovich, S. Ya. (1968). Diffraction of Plane Waves by a Circular Island. Atmos. Oceanic Phys. 4:35-40.

Snodgrass, F. E., W. H. Munk, and G.R. Miller. (1962). Long Period Waves over California's Continental Borderland. Part I. Background spectra. J. Mar. Res. 20: 3-30.

Stokes, G. g. (1846). Report on Recent Researches in Hydrodynamics. Br. Assoc. Rep. 1846: 167p.

Summerfield, W. C. (1969). On the Trapping of Wave Energy by Bottom Topography. Flinders Univ., South Australia, Horace Lamb Cent. Oceanogr. Res., Res. Pap. 30: 214p.

Ursell, F. (1952). Edge Waves on the Sloping Beach. Proc. R. Soc. London Ser. A, 214: 79-97.

Williams, W.E. (1964). Note on the Scattering of Long Waves in a Rotating System. J. Fluid Mech. 20: 115-119.

Yanuma, T. and Y. Tsuji (1998). Observation of Edge Waves Trapped on the Continental Shelf in the Vicinity of Makurazaki Harbor, Kyushu, Japan. Journal of Oceanography, 54, pp. 9-18.

POTENTIAL OVERLOOKED ANALOGUES TO THE INDIAN OCEAN TSUNAMI IN THE WESTERN AND SOUTHWESTERN PACIFIC

Daniel A. Walker
Tsunami Memorial Institute
59530 Pupukea Road
Haleiwa, Hawaii 96712

ABSTRACT

In a more detailed examination of subducting margins of the Western and Southwestern Pacific, segments are found that are similar to the segment along the Indian Ocean that ruptured on 26 December 2004. Similarities are found in terms of hypocenter distributions and historical seismicity. The largest reported moment magnitudes in the Western and Southwestern Pacific since 1900 were an 8.5, an 8.4, and an 8.3. Should any substantially larger earthquakes occur along these segments or elsewhere in the Western or Southwestern Pacific, Civil Defense agencies in the Hawaiian Islands should be aware of any possible inadequacies in existing evacuation procedures for western and southern shores.

INTRODUCTION

In an earlier report (Walker, 2005) comparisons were made between the seismic histories of the eastern margin of the Indian Ocean and subducting margins of the Western and Southwestern Pacific. From 1900 through 25 December 2004, the largest moment magnitude (Mw) earthquakes at depths of 100 kilometers or less throughout the Western and Southwestern Pacific were an 8.5, an 8.4, and an 8.3. For the same time period and depth range in other areas of the Pacific, the largest values were a 9.6, 9.2, and 9.0. Along the eastern margin of the Indian Ocean for the same time period and depth range, the largest values were two 7.9's. For specific portions of the circum-Pacific arc from Japan southward to New Guinea and eastward from New Guinea to Samoa, seismic histories similar to the eastern margin of the Indian Ocean were found.

Using data prior to 26 December 2004, earth scientists could have concluded that significant ocean-wide tsunamis in the Indian Ocean were not a likely occurrence. Facing other serious political, social, and economic issues, public officials in countries surrounding the Indian Ocean could easily use the historical record prior to 26 December 2004 as justification for assigning a low priority to concerns for a devastating ocean-wide tsunami. In this report a more detailed analysis of specific segments of the circum-Pacific arc to the west and southwest of the Hawaiian Islands are investigated as possible analogues to the eastern margin of the Indian Ocean. Such investigations should be of interest because, as in the Indian Ocean, no significant Pacific-wide tsunamis (Table 1) are known to have been generated from that portion of the circum-Pacific arc extending from south of Japan to Samoa. Therefore, earth scientists might similarly conclude that such areas are unlikely source locations for significant ocean-wide tsunamis; and public officials could assign a low priority to concerns for a devastating ocean-wide tsunami from those regions.

ANALYSIS

Hypocenter distributions (i.e., epicenters for two depth ranges) for the eastern margin of the Indian Ocean are shown in Figure 1. These data are taken from the U.S. Geological Survey's National Earthquake Information Center (NEIC) on-line data base for magnitude 5.5 or greater earthquakes from 1973 through 25 December 2004. [The magnitude range and time period used provides for reasonably accurate hypocenter determinations.] Also, since only shallow or intermediate focal depth earthquakes have generated significant ocean-wide tsunamis (Table 1), only hypocenters for focal depths of 70 kilometers or less are shown in Figure 1. In many areas the shallower earthquakes (i.e., 33 km or less) are distributed across the subducting margin on either side of the deeper intermediate events (i.e., 70 km to 33 km). The frequency distribution of moment magnitudes from 1900 through 25 December 2004 for earthquakes with focal depths of 70 kilometers or less in the area shown in Figure 1 is given in Table 2. The largest earthquake in the 104 years prior to the 9.0 Mw event (NEIC reported Harvard solution) on 26 December 2004 was a 7.9.

Figure 2 provides additional evidence that significant tsunamigenic earthquakes generally have focal depths of 70 kilometers or less. Figure 2 is a hypocenter plot for the 48 hour time period from 25 December 2004 through 26 December 2004. The depth range for this NEIC data search is 0 to 800 kilometers and the magnitude range is 1 to 10. In separate NEIC listings of these 287 earthquakes (not shown), none were found for the 25th of December. The first earthquake to appear on the list was the 9.0 Mw 30 kilometer depth event at 00 hours and 58 minutes on the 26th followed by 286 earthquakes in the next 23 hours. None of these had a focal depth in excess of 70 kilometers, the greatest reported depth being 61 kilometers. These data indicate substantial decoupling between deeper structures and the displacements occurring at depths of 70 kilometers or less. Decoupling is further indicated by a longer term analysis of NEIC data. In the month prior to the 26th, four earthquakes with depths in excess of 70 kilometers were found. In the month including and following the 26th, two earthquakes with depths in excess of 70 kilometers were found.

An overview of subducting margins throughout the Western and Southwestern Pacific is provided by the hypocenter distributions shown in Figure 3. Hypocenter distributions for a specific segment south of Japan are shown in Figure 4. In many areas shallower earthquakes are distributed across the subducting margin on either side of the intermediate events. The distribution of moment magnitudes from 1900 through 2005 is shown in Table 2. The largest values are two 8.1's. [It should be noted that the Sanriku earthquake of 1933 occurred to the north of the area shown in Figure 4 at 39.2N and 144.5E. This earthquake had a magnitude of 8.4 and a maximum reported runup in the Hawaiian Islands of 3.3 meters (Table 1).]

Hypocenter distributions in the Solomon Islands are shown in Figure 5. Again in many areas shallower earthquakes are distributed across the subducting margin on either side of the intermediate depth events. From 1900 through 2005 the largest earthquake is an 8.1 (Table 2). [Note that in some regions, islands just to the north of possible source locations might impede the transmission of tsunamis into the Pacific.]

Hypocenter distributions for Vanuatu are shown in Figure 6. Again in many areas shallower earthquakes are distributed across the subducting margin on either side of the intermediate depth events. From 1900 through 2005 the largest earthquakes were two 7.8's (Table 2). [Note that numerous island chains (the Marshall, Gilbert, Phoenix, Tuvalu, Kiribati, and Samoa islands) are in the paths of potential tsunamis traveling from either Vanuatu or the Solomon Islands to Hawaii. These islands and their shallower waters may or may not absorb significant amounts of tsunamigenic energy.]

IMPLICATIONS FOR THE HAWAIIAN ISLANDS

In terms of the frequency of large earthquakes, hypocenter distributions, and the extent of apparently contiguous segments (on the order of 1000 km), there are no outstanding distinctions between the segments shown for the Western and Southwestern Pacific and the segment in the Indian Ocean that ruptured on 26 December 2004. Although there may be other factors in assessing the risks of a 9.0+Mw earthquake in the Western or

Southwestern Pacific, the simple analysis presented here should be sufficient for Civil Defense agencies to urgently consider their preparedness for such an event – lest they fall victim to some of the same human failings that contributed to the Asian tsunami disasters. At present, tsunami preparedness in the Hawaiian Islands is based in large part on historical runup data from large tsunamis originating in the North Pacific and South America. Measured runups of 5 to 16 meters for the world's largest recorded earthquakes (9.6 Chile, 9.2 Alaska, and 9.0 Kamchatka; Table 1) and the anomalous 1946 Aleutian tsunami most likely represent worst case scenarios for northern and eastern shores of the Hawaiian Islands. As such, Civil Defense may have enough data to prepare for future tsunamis striking those areas. Since the largest tsunami to strike the Hawaiian Islands from the Western or Southwestern Pacific could be considered to be the tsunami generated by the previously mentioned 8.4 Sanriku earthquake of 1933 (actually located somewhat to the northwest of Hawaii), the following questions need to be asked:

> " Just as the 5 to 16 meter runups on the northern and eastern shores of the Hawaiian Islands were generated by the 9.0+ earthquakes in Chile, Alaska, and Kamchatka, could 9.0+ earthquakes in the Western or Southwestern Pacific generate 5 to 16 meter runups on the southern and western shores of the Hawaiian Islands? If so, is the State prepared for 5 to 16 meter runups in those areas?"

 [A possible consideration in answering these questions is the fact that all known 9.0+ earthquakes (i.e., the Chile, Alaska, Kamchatka, and 26 December 2004 Indonesia earthquakes) have generated ocean-wide tsunamis of at least 5 meters or more. The only other suspected 9+ Mw earthquakes prior to 1900 are the Cascadia earthquake of 1700 that may have generated a 3 meter tsunami in Japan ("USGS Historic Worldwide Earthquakes" on-line data) and the 1868 Chile earthquake that generated a 4.5 meter tsunami in Hawaii ("Historical Tsunami Database for the Pacific, 47 B.C. – 2001" on-line data).]

CONCLUSIONS

  Numerical modeling of tsunamis generated by potential 9.0+ earthquakes for the segments suggested here or for other locations in the Western and Southwestern Pacific is needed to determine the extent of possible inundation in the Hawaiian Islands – especially along western and southern shores. Implications elsewhere throughout the Pacific should also be investigated.

ACKNOWLEDGMENTS

REFERENCES

Hanks, T. C., and H. Kanamori (1979). A moment magnitude scale, J. Geophys. Res., 84, 2348 - 2350.

Lander, J. F., and P. A. Lockridge (1989). United States Tsunamis (including United States possessions) 1690 - 1988, National Geophysical Data Center, Publication 41-2, Boulder, Colorado.

Pacheco, J. F., and L. R. Sykes (1992). Seismic moment catalog of large, shallow earthquakes, 1900 - 1989, Bull. Seismol. Soc. Am., 82, 1306 - 1349.

Walker, D. A. (2000). Twentieth century Ms and Mw values as tsunamigenic indicators for Hawaii, Sci. of Tsunami Hazards, 18-2, 69 - 76.

Walker, D. A. (2005). Critical evaluations for the State of Hawaii subsequent to the 26 December 2004 Asian tsunami, Sci. of Tsunami Hazards, 23-1, 17 - 24.

TABLE 1

SIGNIFICANT PACIFIC WIDE TSUNAMIS
1900 – 2005

Year	Source Location	Magnitude (Mw)	Depth (km)	Runup (m)
1906	Ecuador	8.5	25	1.8
1906	Chile	8.5	25	3.6
1918	Kurils	8.2	25	1.5
1922	Chile	---	25	2.1
1923	Kamchatka	8.5	40	6.1
1933	Japan	8.4	25	3.3
1946	Aleutians	8.0	50	16.4
1952	Kamchatka	9.0	40	9.1
1957	Aleutians	8.6	33	16.1
1960	Chile	9.6	60	10.7
1964	Alaska	9.2	23	4.9
1965	Aleutians	8.7	36	1.1

Significant tsunamis are considered to be those originating on the margins of the Pacific with runups of 1 meter or more in the Hawaiian Islands. Runups listed are the highest reported values from Lander and Lockridge (1989) and Walker (2000). Moment magnitudes are taken from Pacheco and Sykes (1992) using Mw = [log(Mo) – 9.1] / 1.5 (Hanks and Kanamori, 1979). Depths are taken from the U.S. Geological Survey's National Earthquake Information Center (NEIC) on-line data base. The only other earthquake generating runups of 1 meter or more at ocean-wide distances having a reliable focal depth determination is the 9.0 Mw 26 December 2004 Indonesian earthquake with an estimated depth of 30 kilometers (NEIC on-line data).

TABLE 2

MOMENT MAGNITUDES FOR SEGMENTS OF SUBDUCTING MARGINS FOR LOCAL DEPTHS OF 70 KILOMETERS OR LESS

Moment Magnitude	Region			
	Indonesia	S. of Japan	Solomons	Vanuatu
7.0	X		XX	XXXX
7.1	X		XX	XXX
7.2		X	XXXX	XXXX
7.3	XXX		XX	X
7.4	XXX	XXXX	XX	
7.5	XX	XX	XXXX	X
7.6			XXXXX	
7.7	X		XX	XX
7.8	X		XXX	XX
7.9	X	X		
8.0				
8.1		XX	X	
8.2				

The time period for the Indonesia data is 1900 through 25 December 2004. The time period for the data used in other segments is 1900 through 2005. Moment magnitudes through 1989 are taken from Pacheco and Sykes (1992) and Hanks and Kanamori (1979) as indicated for Table 1. After 1989 the values used are the Harvard solutions from the NEIC on-line data base.
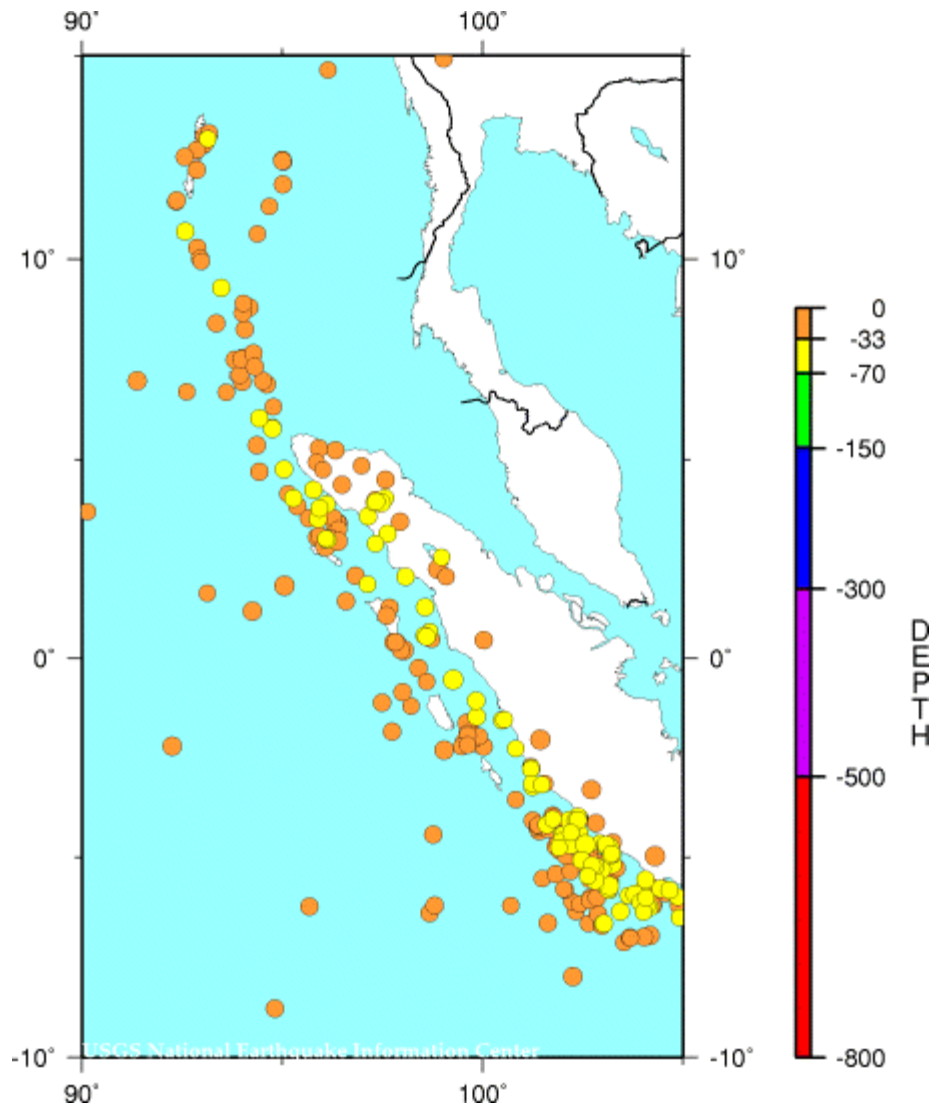
Figure 1. Hypocenter distributions for the eastern margin of the Indian Ocean for focal depths of 70 kilometers or less and magnitudes (i.e., any values: Mw, Ms, mb, or Me) of 5.5 or greater from 1973 through 25 December 2004 using the U.S. Geological Survey's National Earthquake Information Center (NEIC) on-line data base.
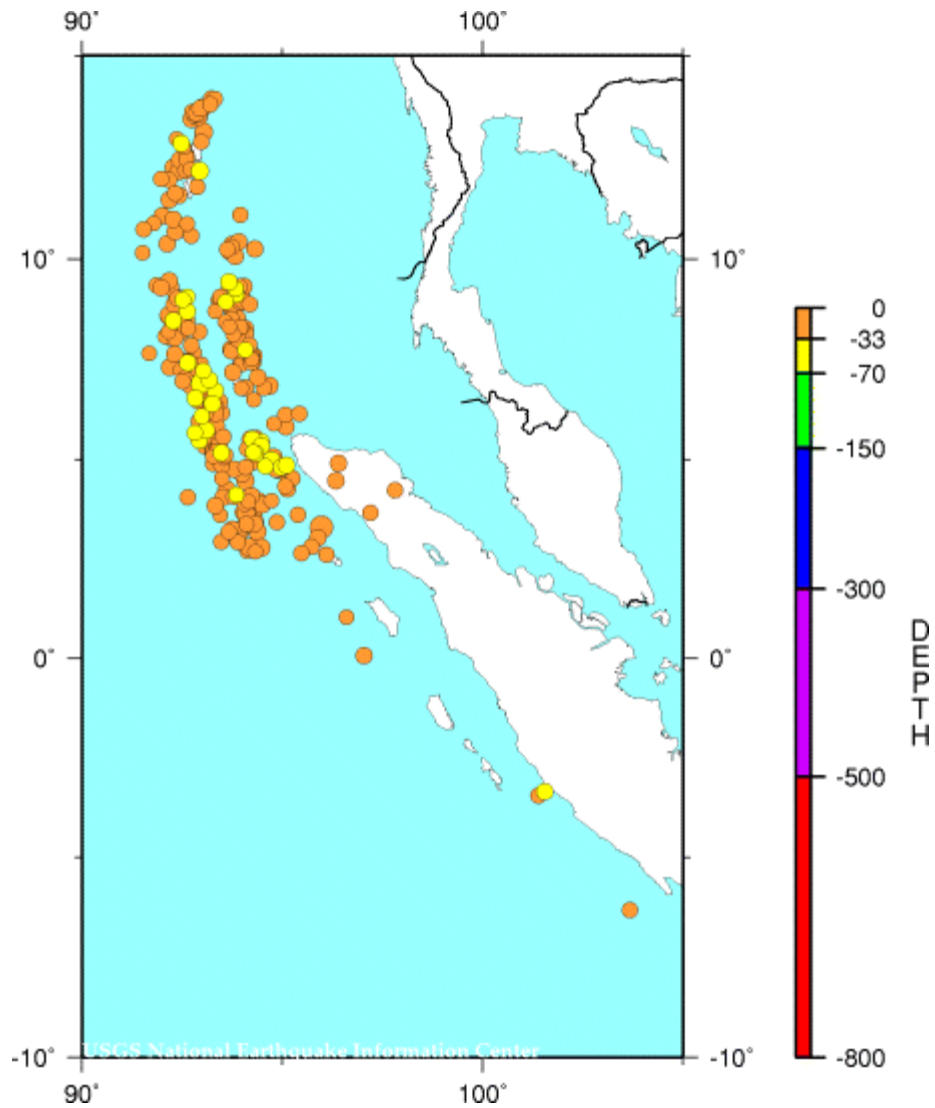
Figure 2. Hypocenters for the eastern margin of the Indian Ocean for all focal depths and magnitudes for the 48 hours from 25 December 2004 through 26 December 2004 using NEIC on-line data.
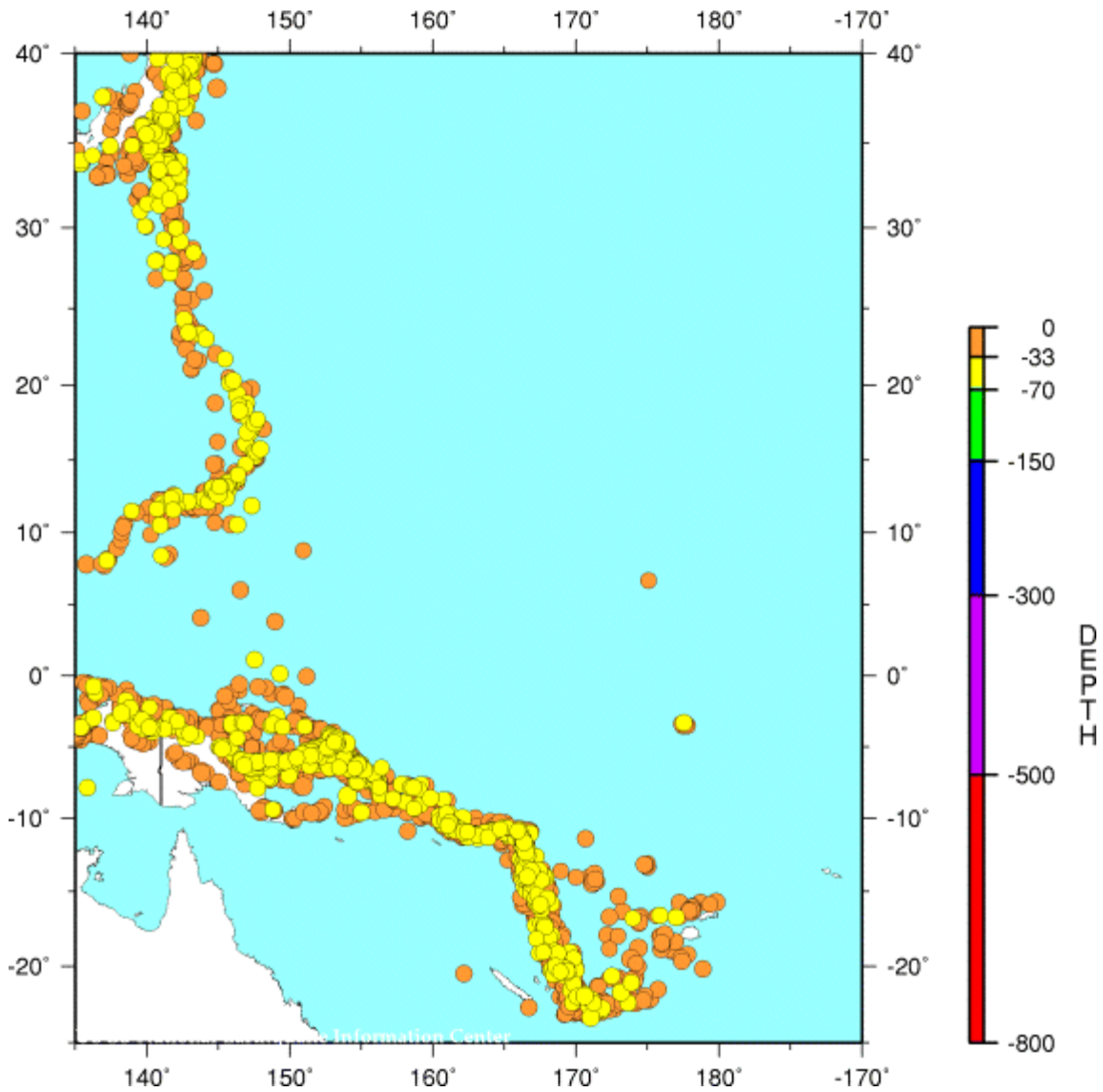
Figure 3. Hypocenters for the Western and Southwestern Pacific for focal depths of 70 kilometers or less and magnitudes of 5.5 or greater from 1973 through 2005 using NEIC on-line data. Similarly restricted NEIC on-line data are shown in Figures 4, 5, and 6.
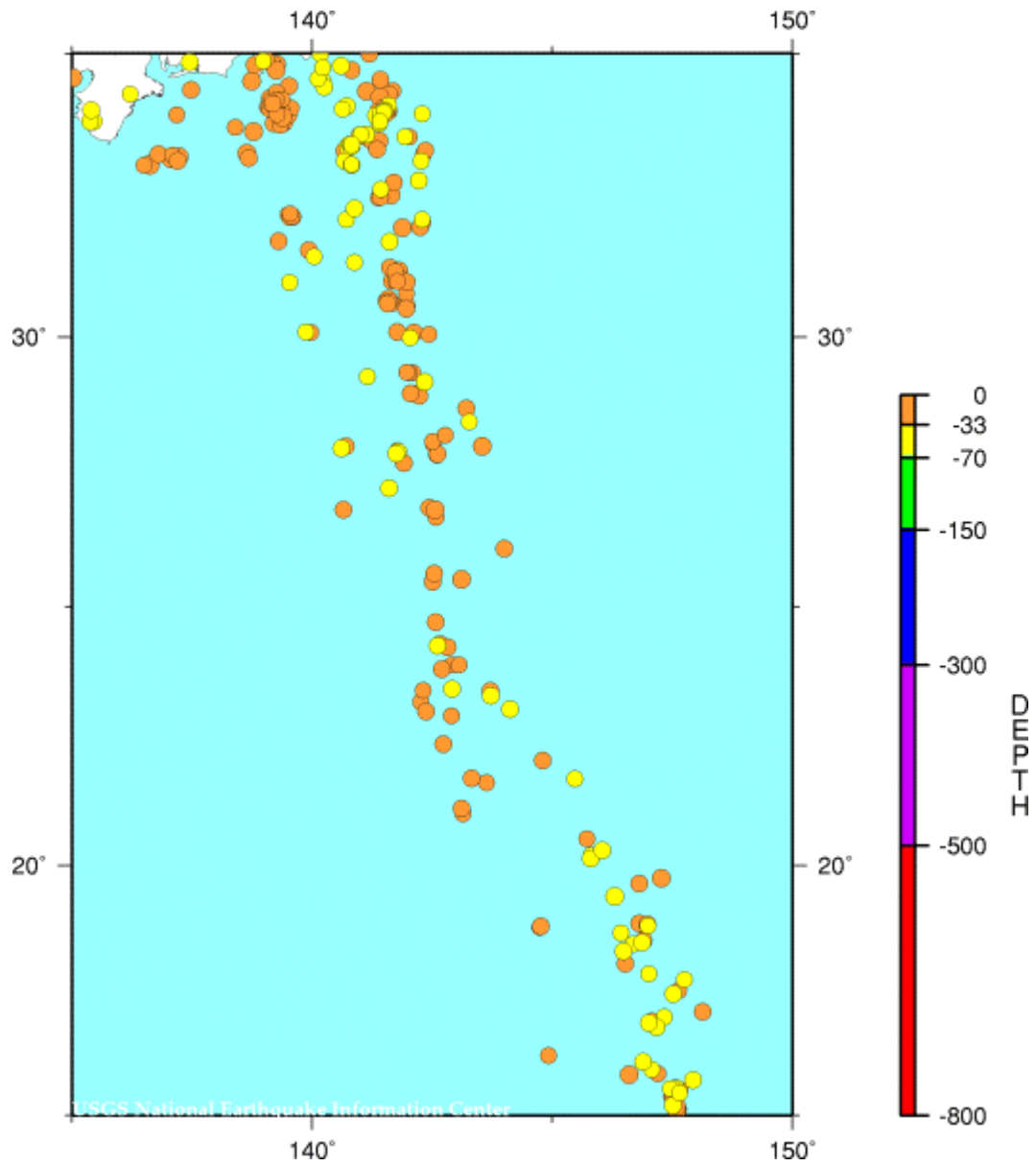
Figure 4. Hypocenters for a segment of the circum-Pacific arc from south of Japan to north of Guam.

Figure 5. Hypocenters for the Solomon Islands.

Figure 6. Hypocenters for Vanuatu.

EFFECTS OF THE DECEMBER 2004 TSUNAMI

AND DISASTER MANAGEMENT IN SOUTHERN THAILAND

Chanchai Thanawood, Chao Yongchalermchai and Omthip Densrisereekul

Faculty of Natural Resources

Prince of Songkla University

Hat Yai, Songkhla. 90110. Thailand.

ABSTRACT

A quake-triggered tsunami lashed the Andaman coast of southern Thailand on December 26, 2004 at around 9.30 am local time. It was the first to strike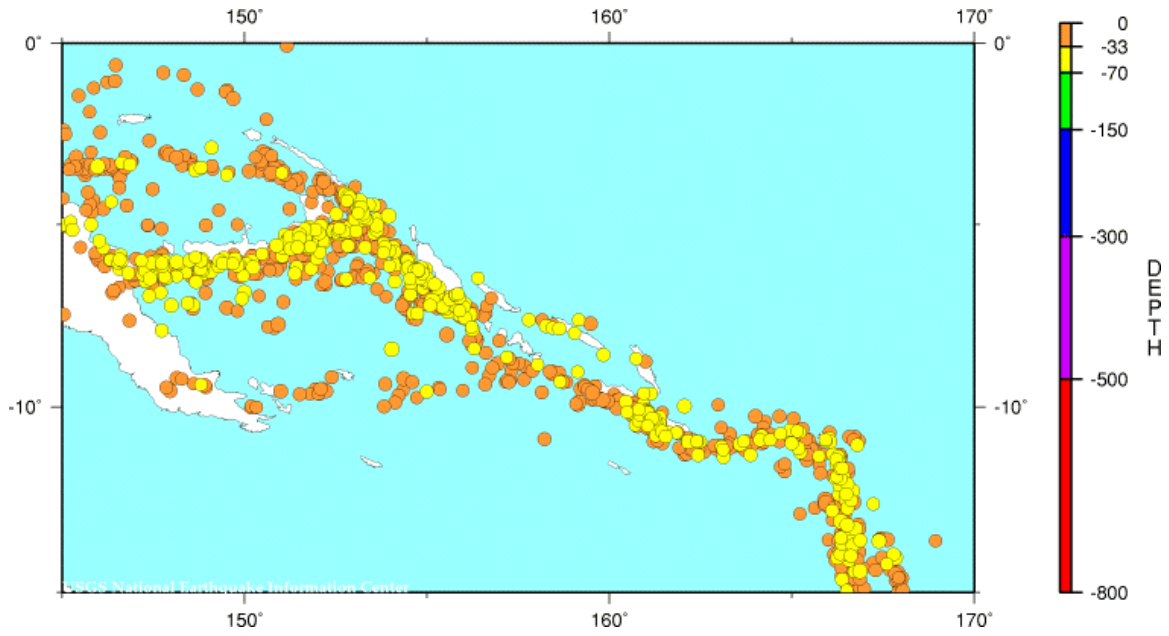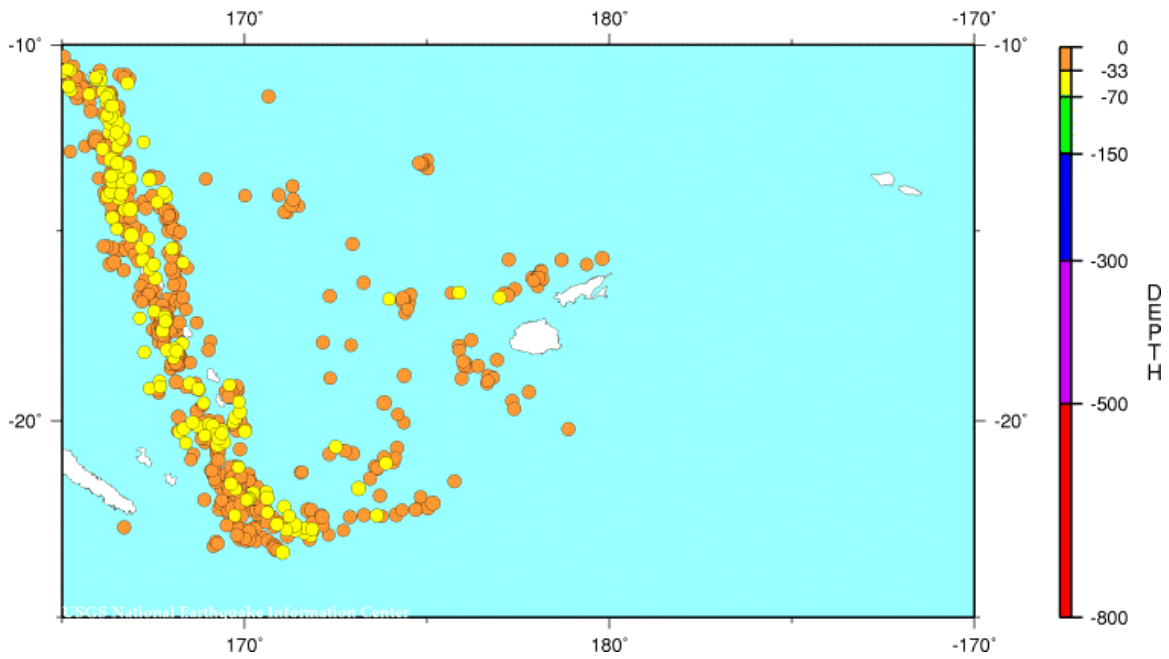 the shorelines of southern Thailand in living memory. Coastal provinces along the Andaman coast suffered a total of 5,395 deaths – more than half of whom were foreign tourists, with another 2,822 reported missing. Of the 6 affected coastal provinces, Phang Nga was the worst-hit province with some 4,224 lives lost and 7,003 ha of land area devastated. Takua Pa District, which was a prime tourist area with numerous beach resorts, was the most severely affected area in Phang Nga Province.

Through the use of the aerial photographs and Ikonos images, it was found that 4,738 ha of Takua Pa District's coastal area were affected by the tsunami. The tsunami run-up heights of 7-8, 5-7 and 10-12 metres, were observed at, respectively, Ban Namkhem, Pakarang Cape and Ban Bangnieng in Takua Pa District. The tsunami caused heavy damage to houses, tourist resorts, fishing boats and gear, culture ponds and crops, and consequently affected the livelihood of large numbers of the coastal communities. The destructive wave impacted not only soil and water resources, but also damaged healthy coral reefs, sea grass beds and beach forests. The surviving victims faced psychosocial stresses resulting from the loss of their loved ones, being rendered homeless and fears of another tsunami. The tsunami effects on human settlements, livelihoods, coastal resources, natural environment together with the psychosocial well being of the coastal communities have contributed to the degradation of the coastal ecosystems.

Following the 2004 event, it has become apparent that the country's disaster management strategies need to be strengthened through the implementation of mitigation and preparedness options to enhance the community's resilience to natural events such as tsunami. The improved strategies are discussed in this paper.

1. INTRODUCTION

Southern Thailand, also designated as Peninsular Thailand, lies between latitudes 5^0 and 11^0 N, and longitudes 98^0 and 102^0 E. It covers an area of 7,153,917 ha and has over 2,705 km of shoreline. The mountain ranges form the backbone of this region, with the western coastline facing the Andaman Sea and the eastern coastline facing the Gulf of Thailand. Many so-call pocket beaches with short and narrow sandy beach nestled between head lands are found along much of the Andaman coast, whereas the Gulf of Thailand coast is characterized by long mainland beaches with associated landforms such as barriers, spits and sand dunes (Sinsakul, 2004). The peninsular area affords excellent access to the seas, with 12 of the 14 southern provinces having sea access. Southern Thailand, in general, enjoys a tropical climate that provides good moisture and humidity throughout the year. Its coastal areas are diverse, and contain productive ecosystems that sustain a large proportion of the coastal population, with plentiful flora and fauna. Pristine tropical rain forests on the uplands, beach forests and soft white sand beaches along the coastal shores and stunning marine life make Thailand's southern region one of Asia's top choice tourist destinations.

In response to the phenomenal growth of the tourism and fishery, including aquaculture industries, tourist resorts, culture ponds, and aquaculture infrastructure have replaced much of the mangrove and beach forests along the coastal shores (UNEP, 2005). Many of the coastal sand dunes that act as natural barriers against incoming waves have been removed to make way for the construction of beach resorts, walkways and roads. Most of the fisher folks and impoverished local populations that made a living in tourist-related activities live in weakly-constructed and unplanned settlements in low-lying areas close to the shores. As a consequence, the coastal areas of southern Thailand have become highly vulnerable to the occurrence of natural disasters caused by extreme events.

At 0059 GMT on 26 December 2004, a magnitude 9.3 earthquake ripped apart the seafloor off the western coast of northern Sumatra, Indonesia. The sudden vertical rise of the seabed by several meters during the quake displaced massive volumes of water, resulting in a devastating tsunami. This seismic sea wave traveled thousands of kilometers across the Indian Ocean, and ravaged the Andaman coast of southern Thailand at 9.30 am local time. Coastal provinces including Phuket, Phang Nga, Krabi, Ranong, Trang and Satun (Figure 1) suffered a total of over 5,395 deaths–more than
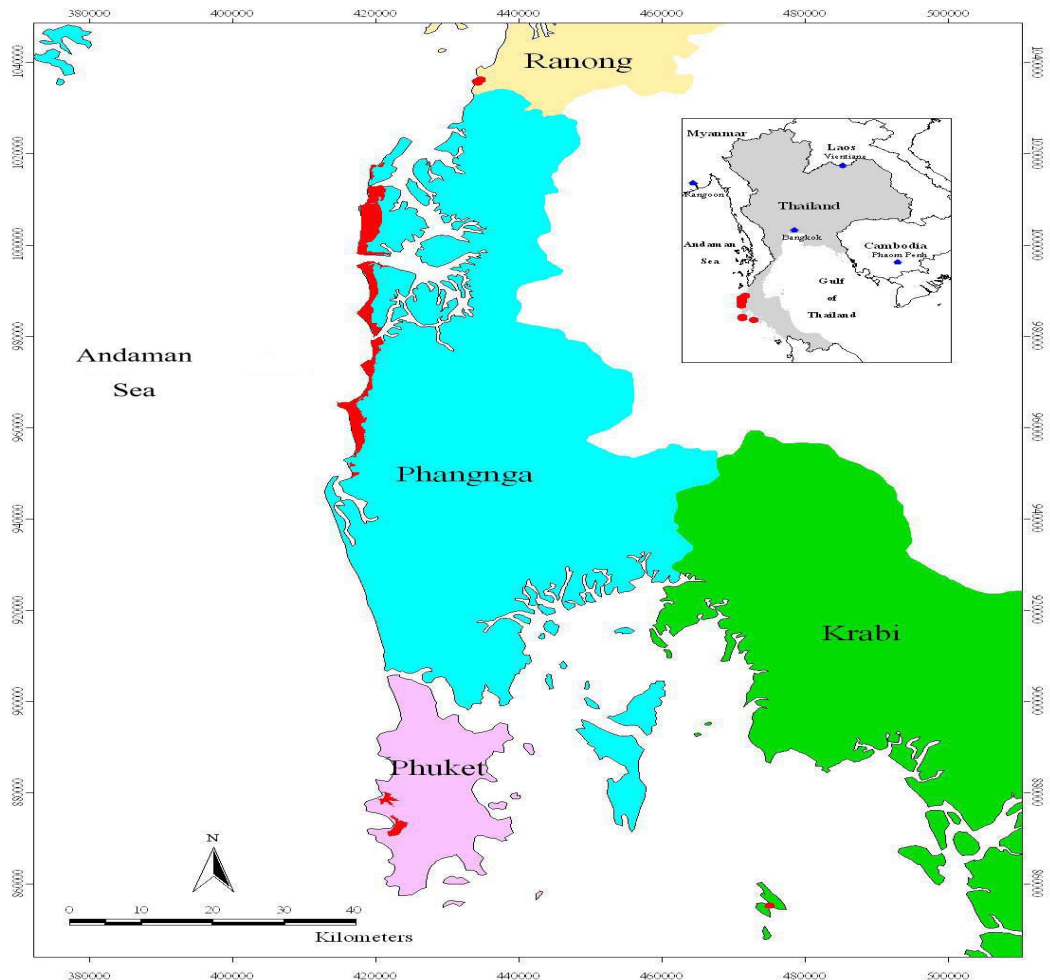
Figure 1. Tsunami affected areas along the Andaman coast, southern Thailand.

half of whom were foreign tourists, with another 2,822 reported missing (Department of Disaster Prevention and Mitigation, 2005). Of the 6 affected provinces, Phang Nga was the worst - hit with some 4,224 lives lost and 7,003 ha of land area devastated. Takua Pa District, which was a prime tourist area with numerous beach resorts, was the most severely affected area in Phang Nga Province (FAO, 2005). In this district, the tsunami destroyed lives, houses, livelihoods on a scale never before seen in Thailand.

As the Indian Ocean has several seismic sources, recurrence of the tsunami on the scale of the 2004 event can be anticipated in the future. According to NGI (2006), a tsunami generated by a magnitude 8.5 earthquake on the Sunda Arc would crash into the Andaman coast of southern Thailand and cause major loss of life and destruction of property again within 50-100 years.

The objective of this study were to (i) assess the effects of the December 2004 tsunami on the coastal ecosystem in Takua Pa District, the worst-affected area in the tsunami tragedy, and (ii) provide recommendations for the strengthening of disaster management strategies to enhance Thailand's capacity to manage a natural catastrophe of the nature and magnitude of the December 2004 event in the future.

2. MATERIALS AND METHODS

This study was based on both primary and secondary sources of data and information. The primary data was obtained through interviews of eyewitnesses, laboratory analysis of soil and water samples, measurement of tsunami run-up heights

and interpretation of remotely sensed data and aerial photographs. The secondary data included information on 2004 tsunami impacts from local government agency offices and sub-district administrative organizations.

2.1 Materials

1) Topographic maps for the tsunami affected area on a 1:50,000 scale, published by the Royal Thai Survey Department in 2000.

2) Colour aerial photographs for the tsunami affected areas on a 1: 25,000 scale, acquired in February 2002, produced by the Royal Thai Survey Department.

3) Ikonos images, pertaining to the affected areas on a 1:4,000 scale, acquired on December 30, 2004, provided by the Geo-Informatics and Space Technology Development Agency (GISTDA).

2.2 Methods

In this study, Geographic Information Systems were used to develop two digitized thematic maps, one which defined the tsunami-affected area boundary, and a land use map of the tsunami devastated area. All GIS computation and coverage overlays were performed with PC ArcInfo software. The boundaries of the area studied were digitized from the 1:50,000 topographic maps. The tsunami affected areas were digitized from a map visually interpreted from the 1:4,000 Ikonos images, acquired 4 days after the December 2004 tsunami event. Land use coverage in the area of concern was generated in ArcInfo format by digitizing from land use maps visually interpreted from the 1:4,000 Ikonos images. The 1:25,000 aerial photographs, acquired in 2002, were used to assist in the classification of land use, and ground truthing was also conducted to validate the final results. Land use types in the tsunami affected areas were determined by overlaying land use coverage with tsunami affected area coverage.

Data on tsunami run-up heights were obtained through interviews of eyewitnesses. Water marks on houses, building and trees provided additional data on tsunami heights. To assess the effects of the tsunami on soil resources, three replicate samples of soil were collected from the worst-hit agricultural area in Takua Pa District, Phang Nga Province at 0-5 and 5-30 cm depths. The soil samples were air-dried, passed through a 2 mm sieve, and analyzed for electrical conductivity (EC) and pH. In addition, three replicate water samples were collected in 0.75 litre polyethylene bottles from the middle of the water column of surface water in the tsunami affected agricultural area in Takua Pa District. The samples were immediately analyzed for dissolved oxygen (DO) using a dissolved oxygen meter. The rest of the water samples were stored on ice and transferred to a laboratory for analyses of salinity and pH.

A field survey was also conducted to assess the impacts of the destructive waves on the psychosocial well being of tsunami affected populations. Takua Pa District, Phang Nga Province was selected for assessment as they experienced many and severe psychosocial problems. Interviews were conducted in a participatory manner with open-ended questions so as to allow the interviewees to guide the outcomes. A total of 128 surviving victims from two coastal sub-districts in Takua Pa District, namely, Bang Mueng and Kuk Khak Sub-districts, were interviewed.

3. RESULTS AND DISCUSSION

Through the interpretation of the aerial photos and Ikonos images, it was found that 4,738 ha of Takua Pa District's coastal area were affected by the devastating tsunami (Table 1). In this district, the affected areas stretched from the coastline of Ban Namkhem, which is located in the north of Takua Pa District close to the border with Myanmar, downward through Pakarang Cape in Ban Bangkaya, which are located in the central part of the district, through Ban Bangnieng, and then to Khao Lak Merlin

Resort, which is located on the coast in the southern part of the district. Of these affected areas, 848 ha or 18.7% were agricultural land, 600 ha or 13.2% were beach forests and 278 ha or 6.1% were urban and built up land (Figure 2 and Table 1). It should be noted that only 7 ha of the mangrove forests in the district were impacted by the tsunami (Table 1).

Based on the field visit, it was evident through interviews of eyewitness and measurements of watermarks on houses, buildings and trees, that Ban Namkhem suffered a tsunami run-up height of 7-8 metres. In this locality, the fishing
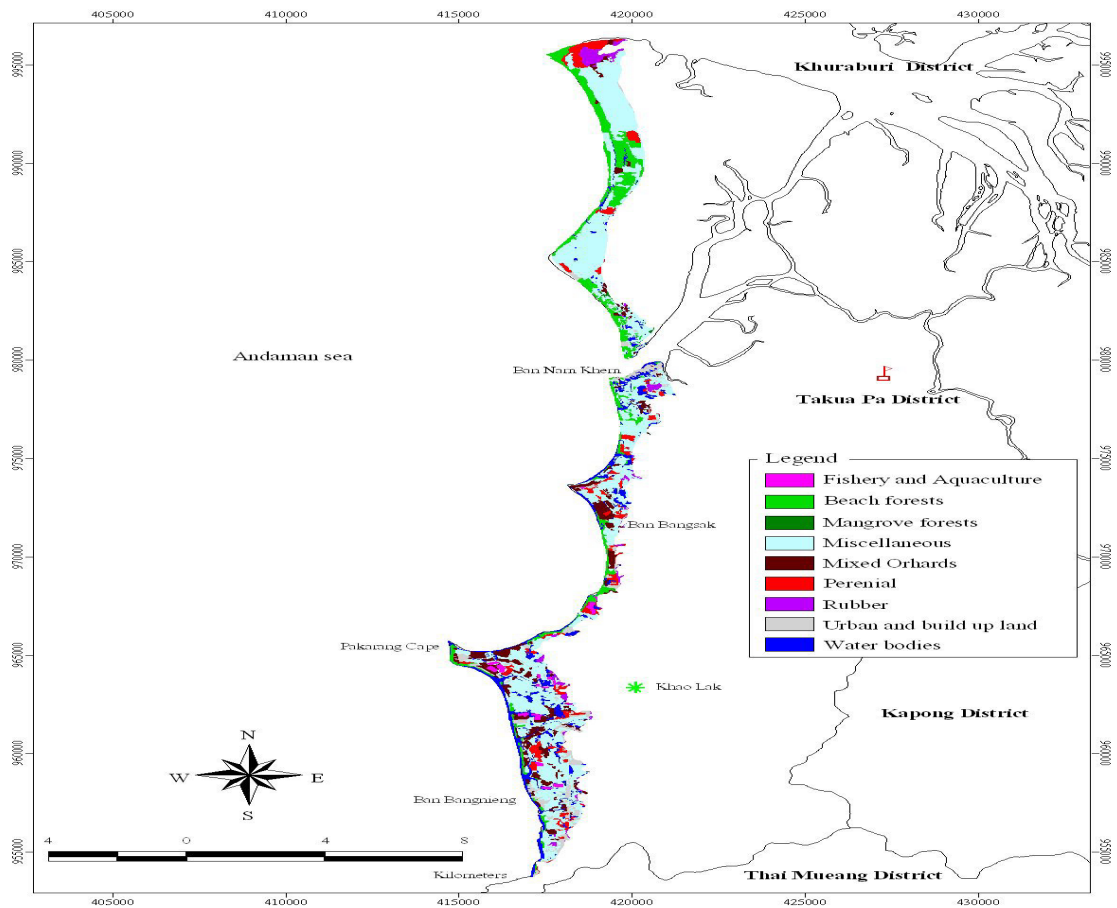
Figure 2 Land use in tsunami affected area in Takua Pa District.

Table 1 Land use types in tsunami affected areas in Takua Pa District.

Land use type	Tsunami affected area	
	Ha	%
1. Urban and built up land	278	6.1
2. Mangrove forests	7	0.2
3. Beach forests	600	13.2
4. Mixed orchard	400	8.8
5. Perennial	316	7.0
6. Rubber	132	2.9
7. Fishery and aquaculture	63	1.4
8. Water bodies	468	10.3
9. Miscellaneous	2,276	50.1
Total	4,540	100.0

communities, living in weakly-constructed houses near sea level, were completely wiped out and lost two-thirds of their inhabitants in the tsunami tragedy. The powerful wave washed away fishing boats and gear, destroyed culture ponds and damaged aquaculture infrastructure. A couple of large fishing boats were even thrown violently inland and deposited in a residential area of Ban Namkhem (Figure 3). At Pakarang Cape, Ban Bangkaya, the maximum tsunami run-up measuring up to 5-7 metres was observed. In this locality, intense beach erosion and severe damage to coral reefs and beach forests were observed (Figure 4), and almost all the luxury hotels and fisher folk villages in close proximity to the seashore lay in ruins. Agricultural land was salinated, and wells and ponds were contaminated with intruding sea water. The powerful wave also damaged coconut and oil palm plantations as trees were uprooted by the action of the wave. The ravages of the destructive wave extended up to 2 kilometers inland.

The tsunami wave of 10-12 metres and inland penetration of wave of 1 kilometres badly damaged Ban Bangnieng, which is one of the important tourist attractions south west of Pakarang Cape. Khao Lak beach, a newly constructed tourist spot, suffered a run-up height of 8-12 meters. The beachfront hotels, tourist resorts and tourism infrastructure along the shore were demolished. At this locality, approximately half of the 400 guests in a luxury beachfront resort perished in the ground-floor rooms, swamped by the force of the giant wave. The loss of life and damage to the property at Khao Lak beach was extensive because the beach was surrounded by elevated ground and hills. With run-up height of 5-6 metres, the tsunami also caused major loss of life and destruction of infrastructure to Khao Lak Merlin Resort. At this locality, the trail of destruction left by the devastating wave extended up to 1 kilometer inland.

Figure 3 A group of resort buildings lies in ruins (left) and a fishing boat rests on shore (right).

Figure 4 Views of the coastal shores in Takua Pa District after the 2004 tsunami.

Prior to the 2004 tsunami, the tourism, fisheries and agricultural industries provided most of the livelihoods in the affected areas along the Andaman Coast. The tourism sector was the most important source of revenue and the biggest provider of livelihoods (UN, 2006). As noted earlier, the field survey conducted after the tsunami revealed that most of the beachfront hotels, tourist resorts and tourism infrastructure in coastal areas of Takua Pa District were totally or partially affected by the catastrophe. Following the powerful tsunami, the fishing industry, including coastal aquaculture, suffered major losses in terms of fishing boats and gear, culture ponds, cages and shrimp hatcheries, thus destroying the local economy.

It was observed during the field visit that the tsunami flooded costal areas up to two kilometers inland. It traveled upstream through coastal estuaries and rivers, extending the devastation well inland from the coast in these areas. Hence, deposition of salts from intruding sea water in soil is expected to occur in the inundated areas. Of seven soil samples collected from the worst-hit area in Takua Pa District in January 2005, six samples at 0-5 cm depths had high EC values (Table 2), rendered it unsuitable for cultivation. Damaged crops included mixed orchards, rubber, oil palms and coconut trees. Likewise, the water quality in wells, ponds and canals in tsunami affected coastal areas was deteriorated due to sea water intrusion as well as sewage-related contamination. Of the six water samples collected from the Takua Pa area, five samples contained high salt levels (Table 3), thereby affecting irrigation options. The impacts of the tsunami on the major economic sectors such as tourism, fisheries and agriculture directly affected the livelihoods of the coastal population.

Table 2 Values of EC and pH of soil samples collected from Takao Pa District

Location	Coordinates	EC		pH	
		0-5 cm.	5-30 cm.	0-5 cm.	5-30 cm.
Ban Nam Khem	0419982 E 0979678 N	4.17	0.81	7.71	6.72
Ban Bangsak	0419390 E 0972754 N	13.94	8.28	8.14	8.66
Kuk Khak Beach	0419362 E 0976550 N	11.67	4.59	9.49	9.20
Ban Kuk Khak	0417119 E 0961439 N	8.28	3.12	8.66	8.73
Ban Pak Veep	0418509 E 0967451 N	6.36	0.83	7.93	6.96
Ban Bangnieng	0417409 E 0958291 N	3.21	2.40	9.13	7.86
Khao Lak Merlin	0416645 E 0948363 N	12.34	8.64	8.25	8.33

Table 3 Values of salinity, DO and pH of water samples collected from Takao Pa District.

Location	Coordinates	Salinity (ppt)	DO (mg/l)	pH
Ban Nam Khem	0419982 E 0979678 N	24.5	4.02	8.19
Ban Bangsak	0419390 E 0972754 N	17.9	6.75	8.35
Kuk Khak Beach	0419362 E 0976550 N	3.70	4.42	7.68
Ban Kuk Khak	0417119 E 0961439 N	24.8	7.17	8.62
Ban Bannieng	0417409 E 0958291 N	28.1	4.59	8.39
Khao Lak Merlin	0416645 E 0948363 N	32.9	4.90	8.06

The field survey also revealed that the December 2004 event also caused substantial deterioration to the natural environment. The destructive wave damaged healthy coral reefs, sea grass beds and beach forests along the impacted coastlines. It was reported, however, that extensive areas of mangroves and other coastal forests had

played an important role in mitigating the effects of the 2004 tsunami disaster (FAO, 2005). The catastrophe also caused significant geomorphologic changes along the Andaman coastline, such as eroding sand beaches and enlarging the mounts of the rivers to the sea (Figure 5). The devastating wave has in fact literally redrawn the shorelines of the Andaman coast of southern Thailand.

Source : Space Imaging/crisp-Singapore.
Figure 5. Pakarang Cape before (left) and after (right) the 2004 tsunami, showing beach erosion.

Through interviews of surviving victims, it was found that the majority of them faced a number of psychosocial stresses resulting from the loss of their loved ones and community members, being rendered homeless, fearful of more tsunamis, suffering from a loss sense of safety and security, and lost livelihoods. For those who survived the tragedy, most of them suffered most from phobic disorders, followed by depressive and anxiety disorders. It will take months and years to restore lives to pre-tsunami levels of functioning. The interview results also showed that many tsunami victims, whose houses were washed away, lost their land ownership right in the aftermath of the tsunami disaster. These critical issues have led to a decline in the quality of life of the affected coastal communities.

The adverse effects of the tsunami catastrophe on coastal resources, natural environment, human settlements, and livelihoods together with a decline in life quality values of the coastal population have contributed to the degradation of the coastal ecosystems. There is therefore a profound need for a rehabilitation of the damaged ecosystems to restore sustainable livelihoods to the people of the affected communities in the coastal areas.

Most of the fatalities along the Andaman coast of southern Thailand can be attributed to the government's failure to warn the coastal communities of the imminent arrival of the tsunami. In fact, thousands of lives could have been saved had a tsunami early warning system been established in the Indian Ocean (Alverson, 2005). Prior to the December 2004 tsunami disaster, there was no operational tsunami warning facility in place in Thailand because the kingdom had never been struck by a tsunami and this type of catastrophic event was considered to be extremely rare in the area (Tibballs, 2005). However, it is still questionable as to how effective this would have been in alerting the coastal communities of imminent danger in a country which has poor communication systems and no awareness of the danger. The lack of precautionary behavior of the coastal inhabitants, even when noticing the suddenly receding tide that

provided a signal of the approaching tsunami, also contributed to the enormous loss of life. It is essential, therefore, to emphasize the urgent need to strengthen and improve disaster management strategies in order to enhance the country's capacity to cope with the impact of future tsunami disaster.

4. TSUNAMI MANAGEMENT STRATEGIES

Although the occurrence of an earthquake and ensuing tsunami cannot be prevented, the magnitude of catastrophic impacts in terms of loss of life and livelihoods, destruction of property and environmental damage can be kept within reasonable limits through an integrated approach to disaster management. Planning for disaster encompasses four different but related aspects, mitigation or prevention, preparedness, response and recovery. In Thailand, however, disaster management has primarily focused on the emergency period response and post-impact recovery. Following the December 2004 tsunami disaster, it has become apparent that such an approach is not sufficient to cope with the threat from the tsunami catastrophe. Much greater emphasis should be given to mitigation and preparedness measures.

In response to the 2004 tsunami, the Thai Government directed the establishment of the National Disaster Warning Centre to function as a centralized unit receiving, monitoring, processing and relaying critical information pertaining to impending natural disasters and issuing a public warning in such an event (UN, 2006). The centre also acts as a national clearing-house of disaster risk management information. In recognizing the fact that disaster response should be based not only on the warning systems, the Thai government has adopted and implemented vulnerability reduction programmes through work in two areas: disaster prevention and/or mitigation to reduce an area's susceptibility to the impact of the tsunami hazards, and preparedness to build tsunami resilient communities. These programmes include the following measures;

1. Mitigation measures.
1.1 Establishment of land use plan for coastal areas based on vulnerability assessments and risk analysis. Critical facilities such as schools, hospital, hotels or high occupancy buildings should not be built in vulnerable areas. Existing tourism facilities, shrimp farms and aquaculture infrastructure located in areas at risk should be relocated.
1.2 Provision of appropriate incentive packages and attractive livelihood opportunities to encourage coastal communities to abandon settling in vulnerable locations and/or living in poor-designed houses, particularly along low-lying areas of the coast.
1.3 Maintenance of environmental and ecological stability of the coastal areas through the enrichment of mangrove and beach forests to act as the first line of defense from tsunami waves (Figure 6), and rehabilitation of lost and degraded coral reefs and sea grass beds to help stabilize the coastline and prevent beach erosion.
1.4 Reconstructing removed coastal sand dunes and protecting the remaining sand dunes to act as a barrier against giant waves. Creating buffer zones along the coastlines to protect coastal communities from tsunami waves are established. The buffer zones or green belts can be created through the establishment of buffer strips of between 300-400 metres, planted with mixed vegetation.
2. Preparedness measures.
2.1 Installation of a local tsunami warning system, which includes siren towers at popular and crowded beaches (Figure 6), and a tsunami warning sensor

floating offshore in the most vulnerable provinces along the Andaman coastline, not only to address the safety and security concerns of the coastal communities, but also to establish southern Thailand as a safe destination for foreign tourists.

2.2 Development of education programme through school and university curricula to educate vulnerable coastal communities about the nature and processes of the tsunami hazard and how to protect themselves at the time of impact as well as the importance of mangrove forests, beach forests and coastal sand dunes in mitigating tsunami effects.

2.3 Formulation of a detailed plan for emergency evacuation of vulnerable coastal communities as well as organizing evacuation drills in order to make the appropriate response more of an instinctive reaction, requiring less thinking during an actual emergency situation.

Figure 6 A tsunami warning tower (left) and re-planted beach forests (right) along the coastal shores.

2.4 Raising the awareness of coastal communities about the dangers posed by a deadly tsunami. Brochures, posters, calendars, and announcements on radio and television can be used to stimulate public awareness.

2.5 Construction of a tsunami memorial to commemorate areas devastated by the 2004 tsunami. The memorial would become a major attraction for both locals and visitors, helping them to understand the coastal geomorphology and ecosystems of the Andaman coastline, and to remind them of the disastrous consequences of the December 2004 tsunami events.

The disaster plans of action, including elements of disaster mitigation and preparedness activities as well as responsible agencies are shown in Table 4. It is essential that attention be given to coordinating and integrating mitigation and preparedness activities implemented by various government departments and non-governmental organizations so that the scarce resources available can be used in the most effective and timely manner. Moreover, local community involvement in planning and implementing the measures of hazard mitigation and emergency preparedness is needed to ensure continued interest and support during the implementation stage.

In light of concerns about the recurrence of the tsunami disaster in southern Thailand, more collaboration between international research communities to pool resources, scientific knowledge and expertise should be encouraged so as to bring about an increase in the capacities of the relevant authorities and vulnerable communities to cope effectively with such eventualities. Examples of research topics that should be undertaken are as follows;

1) Tsunami hazard assessment using Remote Sensing and GIS.

Table 4 Disaster plan, activities and responsible agencies for dealing with natural events.

Disaster plans	Activities	Responsible agencies
1. Mitigation	1.1 Risk assessment and vulnerability analysis.	1.1.1 Academic institutions. 1.1.2 Department of Disaster Prevention and Mitigation.
	1.2 Land use planning	1.2.1 Department of Marine and Coastal Resources. 1.2.2 Department of Town and Country Planning.
	1.3 Enrichment of beach forests, and rehabilitation of coral reefs and sea grass beds.	1.3.1 Royal Forestry Department. 1.3.2 NGOs. 1.3.3 Sub-district Administrative Organization.
2. Preparedness	2.1 Installation of warning system.	2.1.1 National Disaster Warning Centre.
	2.2 Development of education programmes.	2.2.1 Academic institutions and schools. 2.2.2 NGOs.
	2.3 Raising awareness.	2.3.1 Sub-district Administrative Organization. 2.3.2 NGOs.
	2.4 Organizing evacuation drills.	2.4.1 Department of Disaster Prevention and Mitigation. 2.4.2 Sub-district Administrative Organization.
	2.5 Construction of tsunami memorial.	2.5.1 Tsunami affected provinces. 2.5.2 NGOs.
	2.6 Disaster-related research.	2.6.1 Academic institutions.

2) Evaluation of tsunami risk in coastal areas based on hazard analysis and vulnerability assessment.

3) Community-based coastal resource management.

4) Creation of detailed digital terrain maps of coastal areas.

5) Determination of evacuation routes and safe places for the coastal communities to use in the event of an emergency.

6) Identification of less vulnerable areas for human resettlements and/or reconstruction of tourism facilities and aquaculture infrastructure.

7) Formulation of a coastal land use plan for coastal areas of southern Thailand.

8) Waste and wastewater management in tsunami affected areas.

9) Reclamation of arable land affected by sea water.

10) Rehabilitation of land destroyed by the actions of tsunami waves.

For successful implementation of disaster responses, mitigation and preparedness schemes should be integrated into the National Economic and Social Development Plan. Recognizing the difficulties of communications, transport and coordination of operations during times of emergencies, it is essential that responsibilities are decentralized and adequate resources for preparedness activities are

allocated to the disaster management committees established at both provincial and districts levels. It is anticipated that the successful implementation of an array of the aforesaid options through people participation and local institutions will make a significant contribution to the resilience to adverse phenomena of the coastal communities that are so crucial to sustainable development in southern Thailand.

ACKNOWLEDGEMENTS

REFERENCES

Alverson, K. 2005. Watching over the world's oceans. Nature 434 : 19-20

Department of Disaster Prevention and Mitigation. 2005. Tsunami Disaster Situation. May 27, 2005. Ministry of Interior. Bangkok, Thailand. http://hazard.disaster.go.th/overall.php?pack=report_10

FAO. 2005. 2004 Tsunami. Report of joint FAO/MOAC detailed technical damages and needs assessment.

NGI (Norwegian Geotechnical Institute). 2006. Tsunami risk mitigation strategy for Thailand. Executive Summary. 55 pp.

Sinsakul, S. 2004. Coastal erosion in southern part of Thailand. p. 7-26. *In* C. Tanavud (ed.). Proceedings of the International Conference on Environmental Hazards and Geomorphology in Monsoon Asia: Progress in Process Study and GIS Mapping. 20-24 December 2004. Hat Yai, Thailand.

Tibballs, G. 2005. Tsunami. The world's most terrifying natural disaster. Carlton Books, Ltd. London. 128 pp.

UN. 2006. Tsunami Thailand. One Year Later. UN. Bangkok. 118 pp.

UNEP. 2005. After the Tsunami. Rapid Environmental Assessment. UNEP. Bangkok. 140 pp.

WHAT IS THE PROBABILITY FUNCTION FOR LARGE TSUNAMI WAVES?

Harold G. Loomis
Honolulu, HI

ABSTRACT

Most coastal locations have few if any records of tsunami wave heights obtained over various time periods. Still one sees reference to the 100-year and 500-year tsunamis. In fact, in the USA, FEMA requires that at all coastal regions, those wave heights due to tsunamis and hurricanes be specified. The same is required for stream flooding at any location where stream flooding is possible. How are the 100 and 500-year tsunami wave and stream flooding heights predicted and how defensible are they? This paper discusses these questions.

PROBABILITY FUNCTION

The theory of probabilities for extreme events is a well developed subject and is routinely applied to: stream and river flooding, wind pressure, minimum and maximum rainfall, life expectancies, breaking of cables and fasteners and more. The theory and many applications are described in the book by Gumbel[1]. This is an advanced statistics book with lots of definitions and mathematics from which I am extracting a small part of the theory for application to tsunami wave heights. Following Gumbel, I use *f(x)* as the probability density function and *F(x)* as the probability distribution function which Gumbel calls simply the probability function, and I will use the same language. In other words,

$$F(x) = prob(X \leq x)$$

Where X is the random variable, i.e. the result of an experiment or a measurement, and

$$F'(x) = f(x).$$

Let's assume that at a given location there actually is some probability function for wave heights of a series of tsunamis over time, and we want to determine what that probability function is and its parameters. At a given location it is assumed that each maximum wave height for a tsunami event is a realization of a random variable and that all of these random variables are drawn from the same probability function $F(x)$. It is this $F(x)$ that we want to determine. If the collection of n wave heights is arranged according to size, then the variable at each location in the sample has its own probability function, and it is not the same as the overall probability function from which the sample is drawn. This subject is called order statistics. We are interested in the probability function, $F_n(x)$, for the random variable X_n, the largest wave height in the sample. If someone were interested in minimum rainfall or minimum breaking strength, they would be interested in $F_1(x)$, the probability function for the smallest value of the sample. In order for the largest member of the sample to be $\leq x$ it is necessary that every member of the sample be $\leq x$, so

$$F_n(x) = F^n(x).$$

Note that the probability function for the largest value in the sample is different from the probability functions of the individual variables in the sample. Here is where extreme value statistics get interesting. It turns out that there are only 3 asymptotic forms for these extreme value probabilities, depending on whether the probability density functions

---

[1] The book by Gumbel referenced at the end has a bibliography of papers and examples on this subject pretty complete up until the year 1958.

for the individual random variable goes to zero like e^{-x}, like x^{-k}, or is bounded in some way. Note that this is not a limit as $n \to \infty$, (n is a fixed number!) but rather an asymptotic approximation as $x \to \infty$, which is appropriate because it is for large values of x that we want the probability function. If one knew exactly the original probability function one could evaluate $F^n(x)$ for any given x and n. However, even not knowing the original probability function, but reasoning in some way that it should fall off exponentially, or like a power of x, or that the range of x is limited in some way, we can still arrive at the asymptotic probability function for the largest wave height in the sample. In fact, the number n is not required to be known either as will be shown later

Taking first the case where the initial probability function is exactly exponential, we have

$$f(x) = \alpha e^{-\alpha x},$$
$$F(x) = 1 - e^{-\alpha x}.$$

In this case the asymptotic probability function is given by

$$F^n(x) = \left(1 - e^{-\alpha x}\right)^n.$$

The asymptotic value of this expression is given by

$$F^n(x) = \exp(-\exp(-\alpha(x-b))) \qquad (1)$$

Such a double exponential function is surprising. One would never guess it from physical principles, but the above function is derived logically which will be demonstrated. That this is so is similar to the well known fact that

$$\lim(1 - x/n)^n = e^{-x} \quad \text{as } n \to \infty.$$

What follows is not a proof (which can be found in Gumbel, in fact two of them) but rather a simple demonstration that the double exponential is reasonable. First a useful value u_n, the characteristic largest value, is defined as the largest value one would expect in a sample of size n, namely, the value for which $F(u_n) = 1 - 1/n$. If this is in the range where the probability function is approximately exponential, then

$$F(u_n) = 1 - e^{-\alpha u_n} = 1 - 1/n$$

from which

$$(1/n)e^{\alpha u_n} = 1$$

.

Substituting this in the equation for $F^n(x)$, one has

$$F^n(x) = \left(1 - e^{-\alpha(x-u_n)}/n\right)^n$$

which gives the asymptotic expression (1) for $F^n(x)$.

A similar kind of argument works for the other two assumptions about the nature of the original $F(x)$ leading to moving the original probability function up to the exponential level. However, for tsunamis it seems like this first asymptotic expression is most reasonable, so we present only the first one.

So how does one find the 100-year and 500-year wave heights? You make an observational probability function out of the existing data, i.e. $X_1, X_2, ..., X_n$ are arranged in order of size and X_m is assigned the cumulative probability of $m/(n+1)$ so that the plotting points are $(m/(n+1), X_m)$. Gumbel has several sections on the choice of what to use for plotting points and the one chosen seems to be the best decision. Then the chosen form of the true probability function is fitted to this observational probability function by adjusting α and b. α is like a scale factor and b is like the mean. These actually can be estimated from the data according to various statistical formulas, but since we are plotting the data anyway, it is easier to get them from the plot. Normally a change of variable is made so that the plot (if you are using the right probability function) can be fitted with a straight line. With a change of variable we have

$$-\ln(-\ln(F)) = \alpha(x - b)$$

and α is the slope of the line and b is its intercept. Once the line is plotted, one picks off the value of x where $F = .99$ and that is the height of the wave which will be exceeded with probability .01. If an event has probability p of occurring during each time unit, then $\widetilde{T}$, the average number of time units between such events will be 1/p. This is not a given but is the result of calculating the average return time. For this reason the probability paper usually has the probabilities scaled along the bottom axis and $\widetilde{T}$ scaled along the top. Similarly, for the 500-year wave, one picks off the wave height corresponding to $F = 1 - .002 = .998$. One can be suspicious of the 500-year wave prediction because one expects geological changes over that period of time, i.e. the sea level could rise significantly or a period of intense volcanic activity could occur. What the 100-year and 500-year predictions really mean is that given conditions as they are now, the first has a probability of .01/year and the second has a probability of .002/year.

Since the plotted data is scattered about a straight line (hopefully) it is obvious that there is uncertainty in drawing the line and thus in the predictions. Gumbel discusses this and in given instances shows how to calculate these uncertainties. Furthermore, in theory it is

possible that the largest value might lie above the line and might be larger that the wave height corresponding to $F = .01$. In other words, there may be a wave observed in a period of time shorter than 100years that actually exceeds the predicted 100-year wave.

There is a very useful added advantage if you have chosen the asymptotic probability function correctly then you can take the 50-year wave and scale it up to the 100-year wave by a simple arithmetic formula. That is you can scale from any time interval to any other time interval with this formula.

This asymptotic expression for waves with probability p can be used (approximately) to compare maximum wave heights for different time intervals. Suppose that $T_1 = 1/p_1$ and $T_2 = 1/p_2$, then

$$- \ln(- \ln(1 - p_1)) = \alpha(x_1 - b)$$

and

$$- \ln(- \ln(1 - p_2)) = \alpha(x_2 - b).$$

Making use of the series

$$\ln(1 + x) = x + x^2/2 + x^3/3 + \dots ,$$

$$- \ln(1 - p) = p - p^2/2 + p^3/3 - \dots .$$

Since p is small, we can take only the first term of the series, so that the original equations can be written as

$$- \ln(p_1) = \ln(T_1) = \alpha(x_1 - b),$$

$$- \ln(p_2) = \ln(T_2) = \alpha(x_2 - b).$$

Subtracting the first from the second we have

$$\ln(T_2) - \ln(T_1) = \ln(T_2/T_1) = \alpha(x_2 - x_1),$$

so that

$$x_2 = x_1 + (1/\alpha)\ln(T_2/T_1).$$

This is very useful. If $T_2 = 2T_1$, then $x_2 = x_1 + (1/\alpha)\ln(2)$, or $x_2 = x_1 + (.693/\alpha)$.

My first reason for using the extreme value statistics (IUGG, Vancouver 1987)[2] was that it is widely used in many similar situations. Also, it seemed basically right because the asymptotic probability function was the right choice, given exponential fall off of the individual probabilities, no matter what the original probability function was. In continuing to reflect on the matter, some questions arise. First of all, what is the sample of wave heights from which the maximum is chosen? It could be the collection of wave heights in the near vicinity of the reported wave height which would surely be the largest.

I should point out that in the application of extreme value statistics to tsunamis, there is not enough data to really determine what probability function to use. The usual test is that the observed cumulative probability function will lie approximately on a straight line when plotted on the correct probability paper which is in effect, the choice of the correct probability function. However, since we have at most 5 values at any location (and many of those values are questionable) in Hawaii this is not a good test. Therefore the choice of the probability function will be mainly an exercise in logical reasoning.

How about augmenting the data with artificial values from imagined tsunamis? There are no probabilities connected with the imagined tsunamis so that doesn't expand the data for probability calculations. How about extending wave measurements of a given tsunami to places where no measurements were made by creating a numerical model of a given tsunami that agrees well at places where the tsunami was measured? This system, which was used for the FEMA maps has some validity. However, there still are too few data points to decide whether or not a straight line describes them well enough.

If I were to guess what the underlying probability function were for wave heights at any location, I would guess normal or Gaussian[3]. This is based on the Central Limit Theorem which says that a sum of random variables approaches the Gaussian whatever the probabilities of those random variables. In this case think of the many variables such as source size, location, mechanism, and all of the additional factors affecting runup size at any given shore location. Think of these as random variables. It seems that there are enough variables here to assume Gaussian for the total effect. Gumbel has a section in which he establishes that Gaussian qualifies as being essentially exponential so that the first extreme value probability function applies. (The conditions to qualify are actually broader than just falling off exponentially!)

Even if it is so that the probability function for wave heights at each point on the shoreline is Gaussian, the value reported and recorded should be treated as the 1st asymptotic probability function. The reason for this is that the wave height actually reported will be the largest of the wave heights from the immediate vicinity of that location.

---

[2] IUGG Tsunami Symposium, Vancouver, B.C., August 18-19, 1987
[3] We would be focusing on the larger tsunamis being fit to the upper end of the Gaussian probability function since it is probabilities of large tsunamis that we are looking for.

Given that the double exponential probability function for wave height is correct, there is another problem with the prediction of the tsunami wave height with return time 100 years. The following simple calculation will demonstrate the problem. Suppose one has estimated that the wave height h_1 is the height exceeded with probability .01, (or $F = .99$). In other words, *.01* is the probability that if a tsunami occurs, its size will exceed h_1. Suppose that on the average there are 5 significant tsunamis in 100 years. Then the probability that all 5 are less that h_1 is $(.99)^5 = .95$. A larger value h_2 must be found so that $F^5(h_2) = .99$, or $F = \sqrt[5]{.99} = .998$. This would, in fact, be the 500-year wave with probability .002 per tsunami. At the rate of 5 tsunamis/100 years, the probability of a tsunami exceeding h_2 would be $5x.002 = .01$, or on the average, once in 100 years.

The above suggests a scheme appropriate when tsunamis occur rather infrequently, say k per 100 years (based on experience.) Assume that the underlying probability function is the 1st asymptotic probability function. It is necessary to create the $-\ln(-\ln y).vs.x$ graph paper with your computer. The observed probability histogram points for the data from a given location are plotted. At this point you can pick off the values of α and b and solve for x for any value of y using the double exponential probability formula. Or graphically you can pick off the value of x for which $y = (.99)^{1/k}$ which gives the 100-year wave at that location.

How well will these methods predict the 100-year and 500-year waves? Unfortunately, or fortunately, we'll never know!

REFERENCES

Gumbel, E.J., <u>Statistics of Extreme Values</u>, Columbia University Press, 1957

Gumbel, E.J., Statistical Theory of Extreme Values and Some Practical Applications, National Bureau of Standards, Applied Math Series, No. 33

TSUNAMI ON 26 DECEMBER 2004: SPATIAL DISTRIBUTION OF TSUNAMI HEIGHT AND THE EXTENT OF INUNDATION IN SRI LANKA

Janaka J. Wijetunge
Department of Civil Engineering, University of Peradeniya,
Peradeniya 20400, Sri Lanka
(e-mail: janaka@fluids.pdn.ac.lk)

ABSTRACT

This paper examines the impact of the massive tsunami of 26 December 2004 on Sri Lanka by tracing the tsunami height, the extent of inundation and the level of damage along the affected coastal belt. The results of an extensive field survey that was carried out in the east, south and west coasts to record the evidence of water levels left behind by the tsunami clearly indicate non-uniform spatial distribution of inundation along the affected coastline of the country. The tsunami inundation had been significantly greater for most parts of the east and the south-east coastal areas than the south, south-west and the west coasts of Sri Lanka. The results also indicate the possible influence of the coastal geomorphology on the extent of inundation. On the other hand, the measurements suggest maximum tsunami heights of 3 m – 7 m along the east coast, 3 m – 11 m on the south coast, and 1.5 m – 6 m on the west coast.

1. INTRODUCTION

The coastal belts of several Indian Ocean countries including Indonesia, Sri Lanka, India and Thailand suffered massive loss of life and damage to property due to the tsunami unleashed by the great earthquake of moment magnitude 9.3 in the Andaman–Sumatran subduction zone on 26 December 2004. In Sri Lanka, 13 of the 14 districts lying along the coastal belt were affected: the death toll was nearly 40,000 with 15,000 injured and about 89,000 housing units either completely or partially damaged leaving one million people homeless and causing massive disruption to livelihoods. The fisheries and tourism sectors were among the hardest hit with many fishing boats and beach-front hotels destroyed or damaged.

However, it was clear in the immediate aftermath of the tsunami, that the degree of damage along the coastal belt of Sri Lanka was not uniform: some areas suffered more damage, some less, and in certain other areas, often not far away, there was no damage at all. This suggests that the level of vulnerability of coastal communities for future events of tsunami exhibits considerable variation even along a short stretch of the shoreline. Such non-uniform spatial distribution of the degree of destruction and damage to lives and property may be attributed to several factors such as the coastal topography, the population density, the construction standards, the type of land use including the density of vegetation and buildings as well as the variations in the tsunami surge height and its velocity owing to the travel path of the tsunami waves, the width of the continental shelf, the energy focusing effects and the nearshore bathymetry. However, detailed studies are necessary for us to understand and determine the way in which the above factors have influenced the spatial variations in the distribution of the tsunami height, the extent of the overland flow and the degree of consequent damage along the affected coastline of Sri Lanka.

Moreover, such field information when supplemented with further inundation data from other possible scenarios of coastal flooding would help determine the level of vulnerability of the coastal communities around the country to future events of tsunamis as well as storm surges. It must be added that, storm surges, although not potentially as destructive as a major tsunami, can be comparatively more frequent, especially for the east coast of Sri Lanka. Therefore, inundation maps indicating the extent of the coastal strip that would be affected by potential events of both tsunamis and storm surges ought to be prepared, preferably for different recurrence intervals.

Such a risk assessment requires the use of mathematical models to simulate the generation, the propagation across the ocean, and eventually, the overland run-up of hypothetical events of tsunamis and storm surges. However, the reliability of the existing numerical models of tsunami has not been tested sufficiently due partly to the paucity of field data as destructive tsunamis are, fortunately, infrequent. Consequently, evidence of the extent of inundation as well as the tsunami height and the run-up left behind by the tsunami on 26 December 2004 must be traced as such data are invaluable to improve our understanding and predictive capability for tsunami hazards.

Accordingly, two Japanese teams carried out such a field survey in the south-west and the south coasts of Sri Lanka during 4–6 January 2005 (Kawata *et al*., 2005) and 6–9 January 2005 (Shibayama *et al*., 2005), respectively. Thereafter, a team of scientists from the United States (Liu *et al*., 2005) made tsunami height measurements during 9–15 January 2005 at several locations in the east, south and south-west coasts of the country. Subsequently, a team of engineers from the Sungkyunkwan University of Korea carried out a tsunami run-up height survey during 20–26 February 2005 in collaboration with a group of engineers lead by the author from the University of Peradeniya, Sri Lanka (Choi *et al*., 2005). The study was carried out at nearly 25 locations around the country, and was focused on areas that had not been covered by the previous surveys. Thereafter, Sato *et al*. (2005) have carried out a field survey in the west and the south-west coasts during 25 February – 2 March 2005. Subsequently, Wijetunge *et al*. (2005) carried out an extensive filed survey in the east, south and west coasts of Sri Lanka to map the extent of inundation around the affected coastline as well as to estimate tsunami heights at several locations where gaps in data existed. Moreover, Sarma (2005) have also made a limited number

of tsunami height measurements in the north coast from Point Pedro down to Mullaittivu under the direction of the author.

Accordingly, in the following, the present paper utilizes the data available from the above field surveys to examine the distribution of the tsunami height and the extent of inundation along the affected coastal belt of Sri Lanka due to the tsunami of 26 December 2004.

2. METHODOLOGY

The methodology adopted in carrying out the Sungkyunkwan-Peradeniya field survey reported in Choi *et al*. (2005) and the subsequent Peradeniya survey of Wijetunge *et al*. (2005) as well as in processing of data is described in the following. The above field studies covered the east coast of Sri Lanka from Nilaveli down to Trincomalee, and then from Vakaneri through Batticaloa, Kalmunai and Akkarapattu down to Potuvil and Panama; Jaffna peninsula from Thondamannar to Manalkadu; and the west and the south coasts from near Colombo through Galle, Matara and Hambantota to the Yala National Park. It must also be mentioned that this was the first time that measurements of the recent tsunami have been made in the north coastal sector.

The measurements at the selected locations of the affected coastline around the island included tsunami height near the shore as well as the horizontal inundation distance, i.e., how far the wall of water has travelled inland causing significant damage.

The tsunami heights were determined visually based on watermarks and damage on structures and/or trees as well as from eyewitness accounts. The heights and distances were measured using standard surveying instrumentation whilst the corresponding locations were obtained by employing a hand-held Global Positioning System (GPS).

During the survey, elevation of each tsunami watermark was measured relative to the mean swash, i.e., the sea level at the shore. Subsequently, the tide-level adjustment was made with the difference in sea levels at the time of measurement and that at the tsunami attack. The tide data used for this purpose are those given in Tsuji *et al*. (2005) as well as those derived from the tidal constituents given in Admiralty Tide Tables (1999) of The United Kingdom Hydrographic Office. Tide data from Point Pedro, Trincomalee, Galle and Colombo were utilized to adjust the measured tsunami heights from the north, east, south/south-west and west coastal sectors, respectively. It must, however, be added that the tide correction was often not more than ±0.2 m (i.e., less than about 2%-6% of the measured tsunami heights) owing to the comparatively small tidal range around the country.

The eyewitness accounts from the east coast indicated that the second wave was the largest and that it had arrived 10–15 minutes after the first wave. Therefore, the approximate arrival time of the highest wave for the east coast, required for tide correction, was taken as 9.30 hrs. by adding 15 minutes to the estimated arrival time of the first wave. The arrival times of the highest wave for the other coastal sectors were also estimated similarly.

The other important parameter in connection with the tsunami overland flow is the extent of inundation. The extent of significant tsunami inundation was determined based on damage to structures and/ or trees and vegetation, lines of debris and location of wreckage as well as eyewitness accounts of overland flow. At many locations, local people could give reliable information about the maximum tsunami run-up, for example, "water came up to this step of this temple …". The furthest limit of tsunami inundation at about 200 m – 400 m intervals along the coastal belt was obtained in this way by employing a hand-held Global Positioning System (GPS). Subsequently, *ArcInfo* software was employed to transform the GPS records of the longitude and latitude in Geographic Coordinate System with 'WGS 1984' as the datum to Transverse Mercator Pojection with 'Kandawala' as the datum. The projected coordinates of the onshore limit of inundation were then laid on 1:50,000 scale topography maps of the Survey Department of Sri Lanka to obtain the horizontal inundation distance from the zero-elevation contour line.

3. SPATIAL DISTRIBUTION OF TSUNAMI HEIGHTS

We first consider the distribution of the estimated tsunami heights in the significantly affected parts of the coastline around the country in Fig. 1. The measurements of Choi *et al*. (2005) as well as those of Kawata *et al*. (2005), Liu *et al*. (2005), Sarma (2005), Sato *et al*. (2005), Shibayama *et al*. (2005), and Wijetunge *et al*. (2005) are shown.

It must be added that, the Sungkyunkwan- Peradeniya field survey (Choi *et al*., 2005) did not cover the coastal stretch from Nilaveli down to Trincomalee as the US team (Liu *et al*., 2005) had already made measurements there, whilst most parts of the coastline north of Nilaveli towards Mullaittivu and beyond as well as the stretch south of Mutur down to around Kokavillu were, unfortunately, not accessible at that time.

The measurements of Choi *et al*. (2005) and Liu *et al*. (2005) suggest maximum tsunami heights of 3 m – 7 m along the east coast from Nilaweli (~8.66^{o}N) through Trincomalee, Mutur, Vakaneri, Batticaloa, Kalmunai and Akkarapattu down to Potuvil, with an increasing trend towards the south.

Meanwhile, on the south coast, there appears to be considerable variation in the tsunami height with values ranging from less than 3 m to as high as over 11 m. Kawata *et al*. (2005) have made tsunami height measurements at five locations at the city of Galle (~80.22^{o}E), and we see in Fig. 1 that the average tsunami height there is about 4.5 m – 5 m.

The measured tsunami heights in the coastal stretch from Galle to Tangalle are about 4 m – 6 m except at two locations; the measurements of Kawata *et al*. (2005) suggest tsunami heights of over 9 m at Koggala Airport (~80.32^{o}E) and those of Shibayama *et al*. (2005) indicate a maximum water level of only 2.7 m at Polhena (~80.52^{o}E). Moreover, the measurements of Shibayama *et al*. (2005), Liu *et al*. (2005) and Sato *et al*. (2005) clearly indicate considerably high tsunami heights of about 9 m – 11 m at Hambantota, Kirinda as well as in Mahaseelawa and Patanangala beach areas of the Yala National Park (coastal stretch from ~81.0^{o}E – 81.5^{o}E).

On the south-west and the west coasts, the measured tsunami heights show a decreasing trend towards the north. The recorded tsunami heights in the Dodanduwa–Beruwala stretch (~6.1^{o}N–6.5^{o}N) is about 4 m – 5 m barring one location at Kahawa (~6.16^{o}N) where the estimated water elevation is over 10 m according to Kawata *et al*. (2005).

Further, Sato *et al*.'s (2005) measurements indicate tsunami heights ranging between 1.4 m – 2.9 m along the coastal reach from Mattakkuliya in the north of Colombo to the Lansigama beach in Marawila (~6.9^{o}N–7.4^{o}N). The comparatively low tsunami heights in the west coast is not surprising as this part of the coast is largely sheltered from direct tsunami impact and only diffracted waves with less energy could reach there.

Moreover, the measurements of Choi *et al*. (2005) in the accessible parts of the coastline of the Jaffna peninsula indicate tsunami heights ranging from about 3.4 m to 7.6 m. It is interesting to note that Point Pedro at the north-east corner of the peninsula has recorded wave heights of over 7 m whilst that at Manalkadu on the east coast of the peninsula is less than 5 m.

The tsunami height estimates of Sarma (2005) in the coastal stretch from Chempiyanpattu (~9.64^{o}N) down to Nayaru (~9.08^{o}N) suggest comparatively high wave heights of 8 – 10 m at Chempiyanpattu and Uduthurai (~9.58^{o}N). Loss of life and damage to property was also reportedly high at Chempiyanpattu and Uduthurai as well as in the densely populated Mullaittivu city (~9.25^{o}N). However, much less destruction to life and property has been reported at Nayaru and Vadduvakal (~9.31^{o}N). It must be added that the tsunami height measurements of Sarma (2005) were made nearly six months after the tsunami event, and therefore, have had to rely largely on eyewitness accounts.
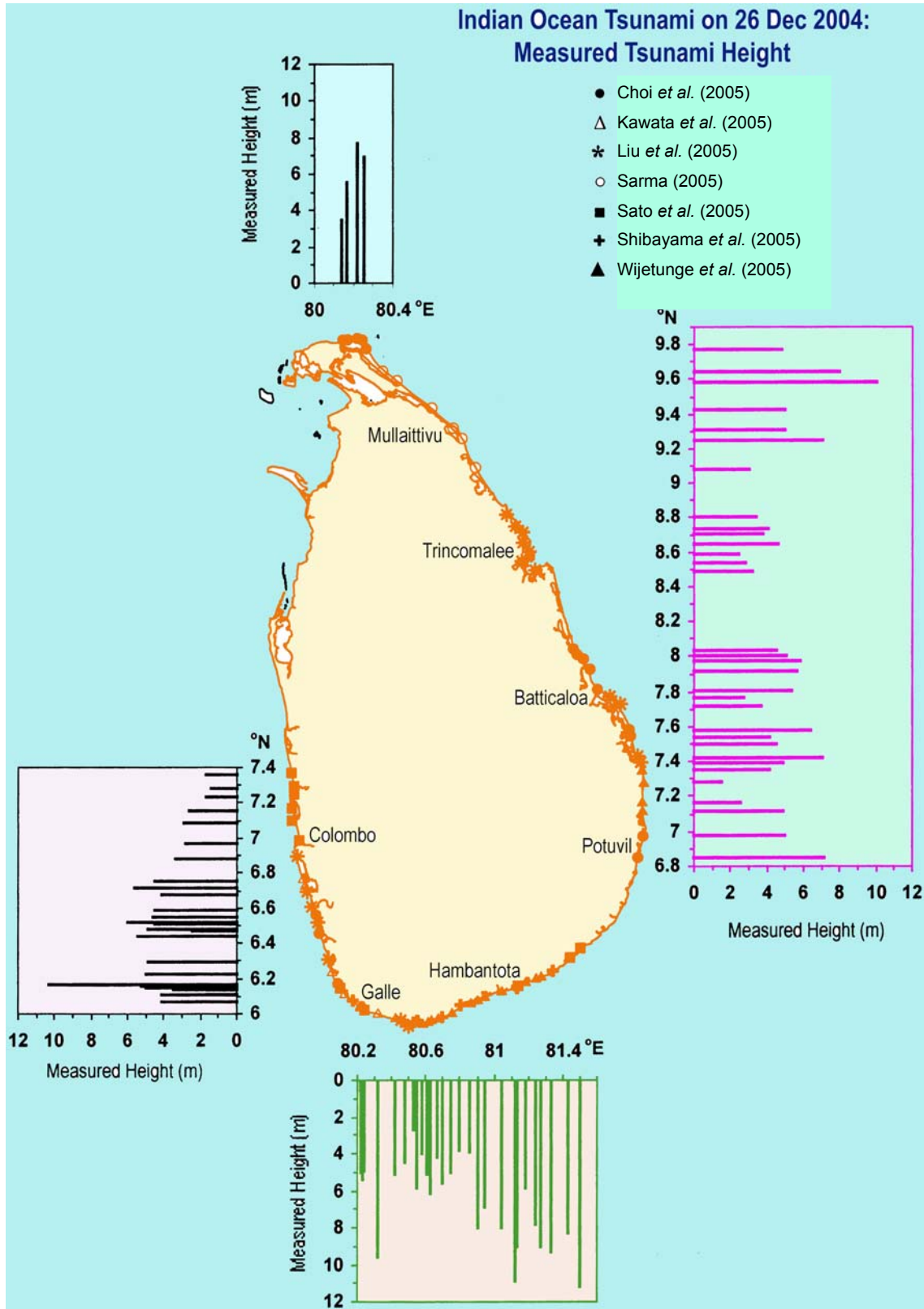
Figure 1. Distribution of tsunami height along the coastline of Sri Lanka.

Fig. 1 also shows that, on the whole, the distribution of the tsunami height along the affected coastline around the country is not uniform. In general, such non-uniform distribution of tsunami height could be attributed to many factors including the travel path of the tsunami waves, the width of the continental shelf, the energy focusing effects, the shape of the coastline and the nearshore bathymetry.

4. SPATIAL DISTRIBUTION OF TSUNAMI INUNDATION

4.1 Coverage

The detailed field investigations carried out by Wijetunge *et al.* (2005) to trace the extent of inundation in Sri Lanka due to the tsunami on 26 December 2006 covered the east coast from Nilaveli through Trincomalee, Kalmunai, Akkarapattu and Potuvil down to Panama; the south coast from Galle through Matara, Tangalle and Hambantota to Yala; and the west coast from south of Colombo down to Galle as shown in Fig. 2. We consider the spatial distribution of the extent of inundation in each of the coastal sectors in the following.
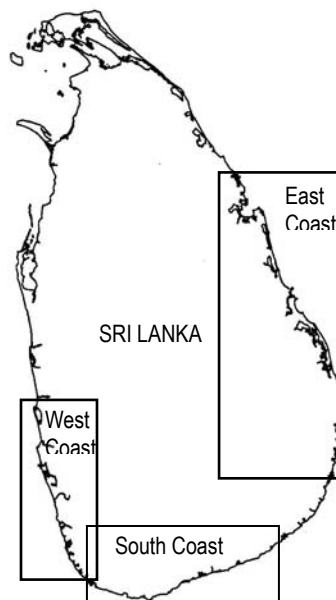

Figure 2. Coastal sectors covered in the inundation survey.

4.2 East Coast

Fig. 3 shows the tsunami inundation distances for the east coast of Sri Lanka together with the estimated tsunami heights for comparison. The two plots give (*a*) the horizontal inundation distance in metres from the shoreline (taken as 0 m MSL), and (*b*) the maximum tsunami water level near the shore in metres above the tide level at the time of tsunami attack (already presented in Fig. 1), against the Northing (N) of that part of the coastline. Note that wherever the spacing between two adjacent inundation measurements is more than 1 km, such data points are connected by a broken line.

The map of the east coast of Sri Lanka also shows the coastal areas with elevation below 10 m MSL. The digital elevation data used in this image are those that were acquired by the Shuttle Radar Topography Mission (SRTM) of the United States National Aeronautics and Space Administration (NASA) in February 2000. The SRTM used Synthetic Aperture Radar (SAR)

technique to capture the land topography, so the actual elevation in some areas could probably be around 7 m – 10 m owing to the possible presence of land cover.
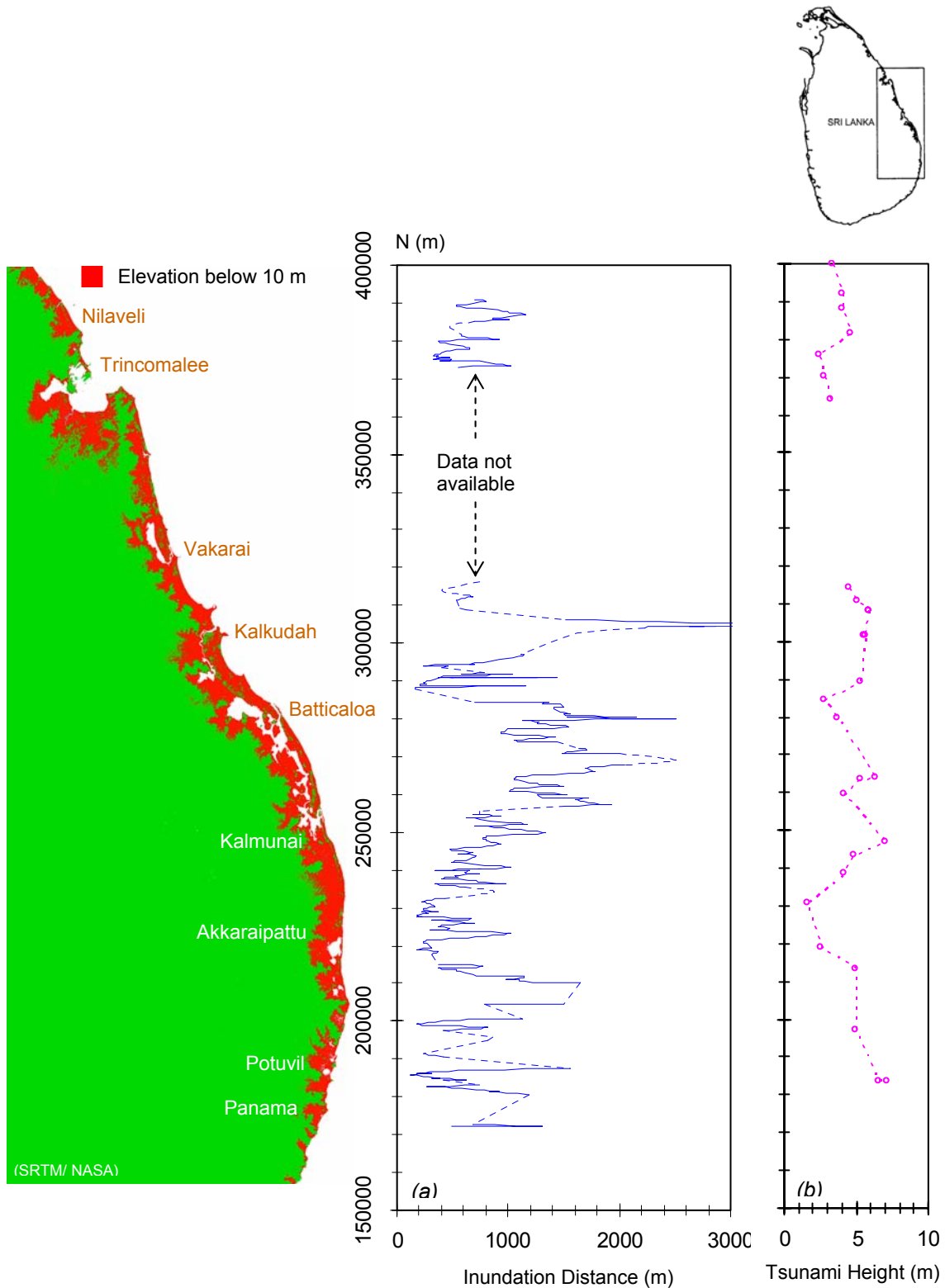

Figure 3. Spatial distribution of (*a*) inundation, and (*b*) tsunami height for the east coast of Sri Lanka.

We see that, on the whole, tsunami inundation had been quite extensive at several locations along the east coast from Nilaveli (~387 kmN) down to Panama (~172 kmN). Such significant inundation peaks, indicating inundation distances of over 2 km, can be seen at Kalkudah (~305 kmN), Batticaloa (~280 kmN), Chuddipalaiyam (~269 kmN) and Kalawanchikudi (~257 kmN). Furthermore, several other locations such as Tirukkovil (~205-210 kmN), Potuvil (~187 kmN) and Panama (~172 kmN) have recorded tsunami penetration distances of 1.5 km – 2 km. In some areas, for instance, around Batticaloa and Kalkudah, the lagoons and other water bodies have certainly helped convey the tsunami surge large distances inland. Moreover, numerous small waterways scattered in the east coast, known as 'Thona' (see Fig. 4), have also helped to carry tsunami surge into settlements interior, which would otherwise not have received tsunami flood waves over the land. In contrast, sand dunes just north of Potuvil (see Fig. 5) have protected some localities from severe flooding due to the recent tsunami.

It is also interesting to note that there is comparatively less inundation of about 200 m at Addalachchenai (~230 kmN) where the maximum tsunami height too is only about 1.5 m – 2 m.

On the whole, a comparison of the inundation peaks with elevation below 10 m areas seems to suggest a strong correlation between tsuanmi inundation and the topography of the land.

It must also be added that the stretch south of Mutur down to around Kokavillu was, unfortunately, not accessible, so inundation and tsunami height data are not available between 320 ~ 360 kmN.

Figure 4. Shore-connected small waterways commonly known as 'Thona' in the east coast.

Figure 5. Sand dunes north of Potuvil in the east coast.

The field observations of damaged boundary walls, brick-mortar type single-storey housing, and multi-storey reinforced concrete framed structures suggested three different failure modes under tsunami loading, namely, overturning, sliding and scouring, as shown in Fig. 6.

(*a*) **Overturning**

(*b*) **Sliding**

Photo: V. Suthagaran

(*c*) **Scouring**

Figure 6. Failure modes of structures under tsunami loading in the east coast of Sri Lanka.

4.3 South Coast

Fig. 7 gives the tsunami inundation distances for the south coast of Sri Lanka from Galle to Yala National Park. The estimated tsunami heights for the south coast are also given in this Figure for comparison.
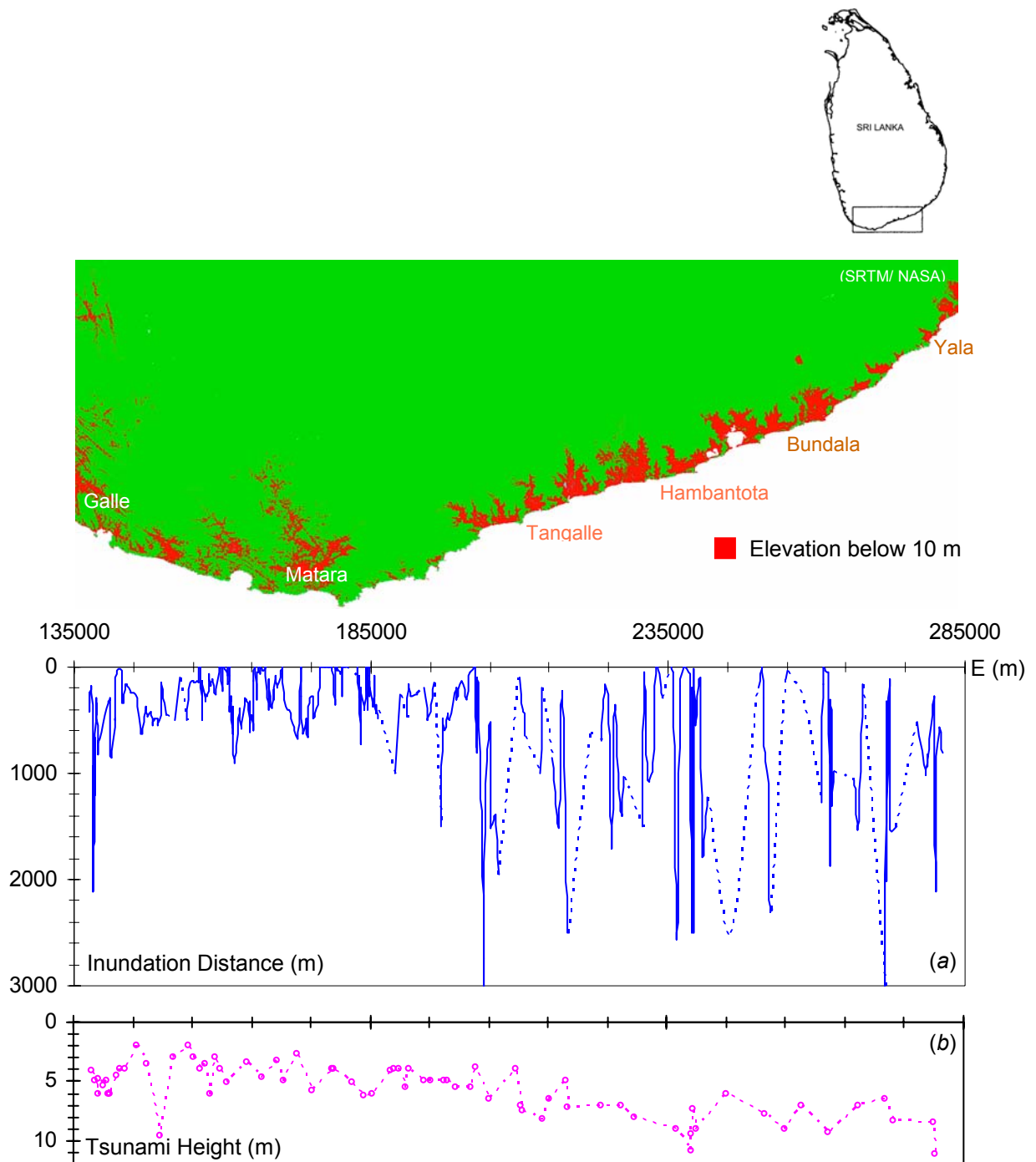

Figure 7. Spatial distribution of (*a*) inundation, and (*b*) tsunami height for the south coast of Sri Lanka.

We see that the deepest tsunami wave penetration in the south coast is at Hambantota, up to three kilometres near the salt-pans, and also near Bundala albeit with the aid of the bay. Significant inundation can also be seen further east of Hambantota, particularly around the smaller lagoons and bays. Hungama-Tangalle beach to the west of Hambantota too has recorded notable inundation, especially where tsunami surge waves had been conveyed inland through water bodies opening to the sea such as lagoons and lakes.

The inundation plot for the south coast shows a stretch of the shoreline without significant tsunami damage between 175 ~ 185 kmE, to the east of Matara. This was not because the tsunami wave heights were low, but because the coastal lands there are at a comparatively higher elevation with steep beach slopes, as observed during the field survey (see Fig. 8) and further confirmed by the topography (elevation above 10 m) map in Fig. 7.

The coastline from Galle to Matara too suffered badly with particularly deep inundation occurring along the coastal belt of Talpe–Koggala–Ahangama (~145 – 150 kmE), besides the tragic loss of life and destruction in the densely populated coastal cities of Galle and Matara.

One prominent feature of the coastal belt from Dickwella (195 kmE) to Yala (285 kmE) is the 7 – 10 m high sand dunes with thick cover of overgrowth (see Fig. 9.). The presence of such sand dunes has certainly helped reduce tsunami penetration inland. However, wherever gaps existed in the dune system, or at locations where the dune height was low or had been cut open for various activities, it appears that the tsunami surge had rushed through with enormous power causing considerable destruction. This was most evident where the popular *Yala Beach Resort* once existed; there, a section of the dune just in front of the resort hotel had been cut open to provide the occupants with a good view of the sea!

Figure 8. Comparatively steep beach fronts east of Matara on the south coast.

Figure 9. Sand dunes near Yala on the south-east coast.

4.4 West Coast

The extent of inundation as well as the measured tsunami heights for the west coast of Sri Lanka from Galle to North of Colombo are shown in Figs. 10*a* and 10*b*, respectively. On the west coast, we see a lessening of tsunami inundation, albeit with intermittent peaks, as we go from Galle to Kalutara and further up. Predominant inundation peaks on this stretch of the coast appear near Paraliya-Telwatte, Akurala, and Balapitiya. Of the several peaks, the most noteworthy is the one near Peraliya where the tsunami surge overturned and submerged a Galle-bound locomotive (see Fig. 11) killing over thousand people. The railway line from Balapitiya to Galle too suffered heavy damage (see, for example, Fig. 12.).

4.5 General Comments

The spatial distribution of the extent of flooding discussed in Sections 4.2 – 4.4 indicate that the tsunami inundation had been greater for the east and south-east coasts than the south, south-west and the west coasts. This was because: (*a*) the earthquake that created the tsunami occurred just about 1000 kilometres east to south-east of Sri Lanka along the Andaman–Nicobar-Northern Sumatra line, so part of the east and south-east coasts had the tsunami waves propagating almost head-on compared to most parts of the south-west and the west coasts which only had diffracted and/ or refracted tsunami waves laterally dispersing into the shadow zone, (*b*) as the tsunami waves crashed almost head-on onto the east and south-east coasts, the velocity and hence the momentum of the tsunami induced surge flow could have been higher resulting in greater penetration along the east coast than the south-west and the west coasts, and, (*c*) the north and the east coasts generally consist of low-lying, wide stretches of flat coastal lands compared to the rest of the country's coastal belt.

It must be added that, what we have discussed above is the larger, overall picture of the tsunami height as well as the resulting inundation and damage for the whole country. However, it was clear during the field surveys that there was considerable local variation of inundation and consequent damage even along a short stretch of the coastline in many parts of the country. In general, such non-uniform tsunami inundation could be attributed to many factors including the nearshore tsunami height, land topography and surface roughness. However, further detailed studies including mathematical simulation of the generation, the propagation across the ocean, and more importantly, the overland run-up of hypothetical events of tsunamis are necessary for us to determine the degree of vulnerability of each locality of the coastal belt of Sri Lanka to potential coastal hazards such as tsunamis and storm surges.
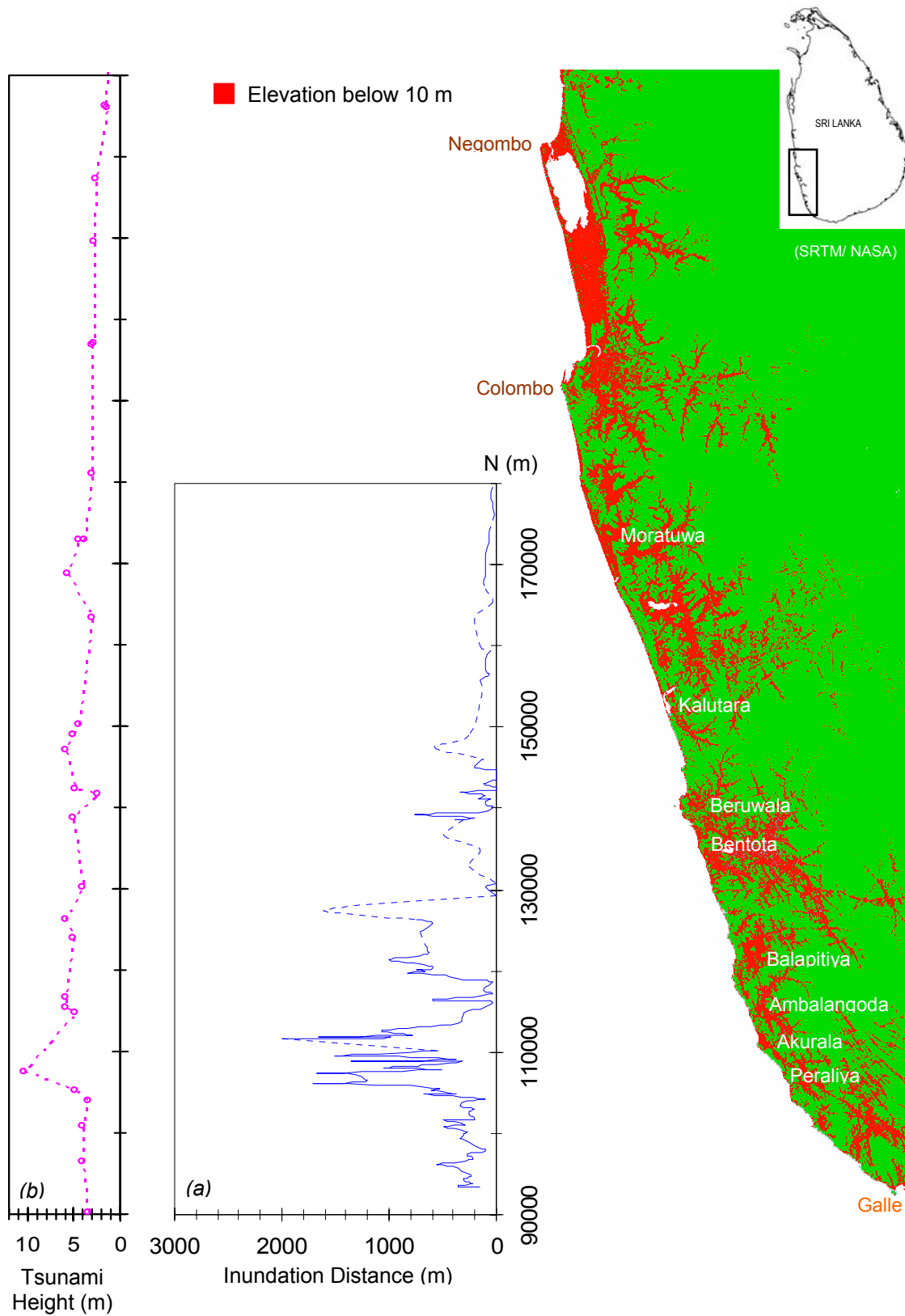
Figure 10. Spatial distribution of (*a*) inundation, and (*b*) tsunami height for the west coast of Sri Lanka.

Figure 11. Overturned rail carriages near Peraliya on the south-west coast.

Figure 12. Heavily-damaged southern railway near Akurala.

5. CONCLUSIONS

The evidence of tsunami height and subsequent run-up left behind by the tsunami on 26 December 2004 has been mapped in the affected coastal belt of Sri Lanka as such data are invaluable to improve our understanding and predictive capability for tsunami hazards.

On the whole, the tsunami inundation had been greater for the east and south-east coasts than the south, south-west and the west coasts of Sri Lanka. The results also indicate the possible influence of the coastal geomorphology on the extent of inundation.

The measurements suggest maximum tsunami heights of 3 m – 7 m along the east coast with an increasing trend towards the south. On the south coast, there appears to be considerable
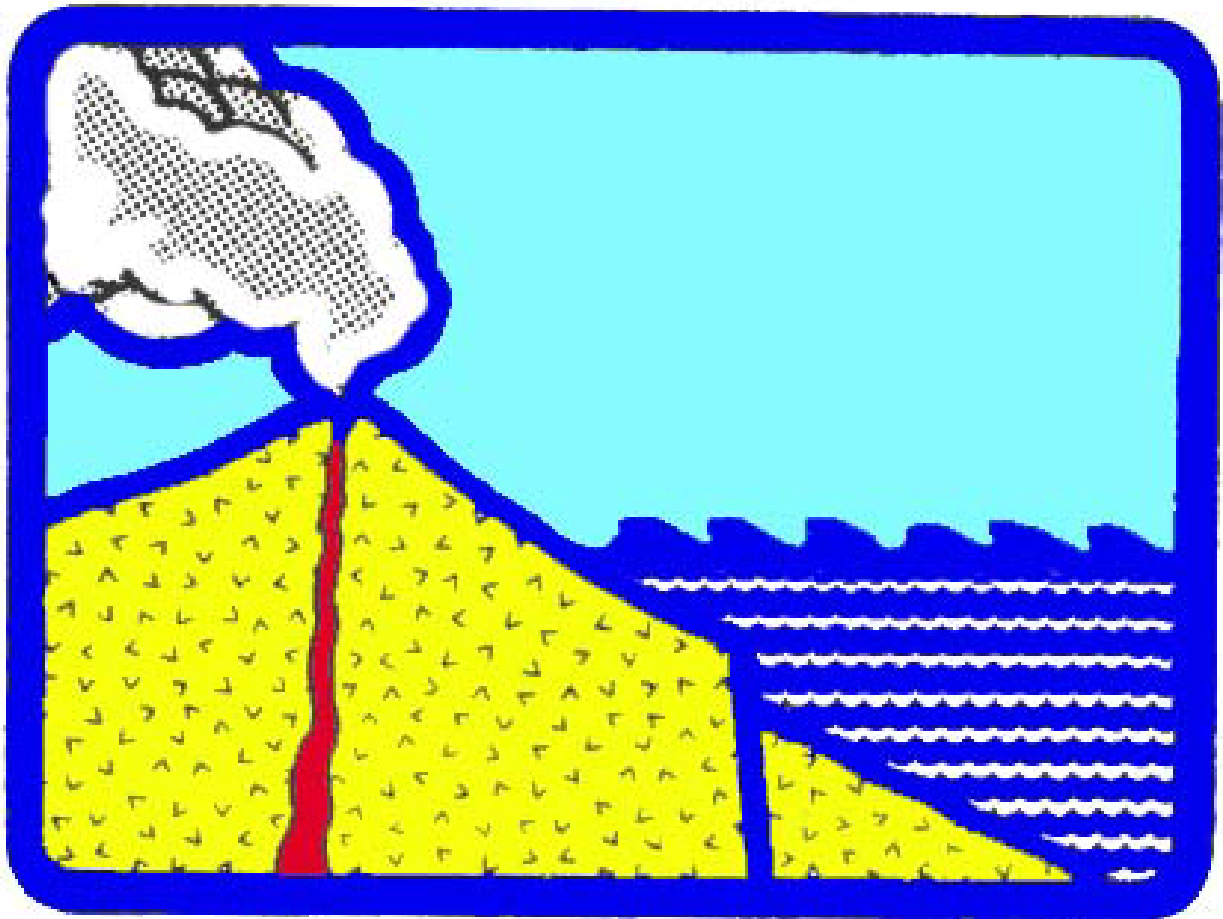
variation in the tsunami height with values ranging from less than 3 m at Polhena, about 5 m at Galle and Matara to as high as over 11 m near Hambantota, Kirinda and Yala. On the west coast, as one would expect, the measured tsunami heights show a decreasing trend towards the north.

ACKNOWLEDGEMENT

REFERENCES

Choi, B. H., Siripong, A., Sundar, V., Wijetunge, J. J., and Diposaptono, S. (2005), "When the sea strikes back: The December 26, 2004 earthquake tsunami of Indian Ocean- Run-up survey". Workshop on Indian Ocean Tsunami, 13th Pacific Ocean and Asian Marginal Seas (PAMS)/JECSS Meeting, Bali, Indonesia.

Kawata, Y, Imamura, F., Tomita, T., Arikawa, T. & Yasuda, T. (2005), "The December 26, 2004 Sumatra Earthquake Tsunami: Field Survey around Galle, Sri Lanka". http://www.drs.dpri.kyoto-u.ac.jp/sumatra/srilanka/galle_survey_e.html.

Liu, P., Lynett, P., Fernando, J., Jaffe, B., Fritz, H., Higman, B., Synolakis, C., Morton, R. & Goff, J. (2005), "South Asia Tsunami, Sri Lanka Field Survey". http://ceeserver.cee.cornell.edu/pll-group/tsunamis_data.htm.

Sarma, A. K. (2005), Personal communication.

Sato, S., Koibuchi, Y., Honda, T., Welhena, T. & Ranasinghe, S. (2005), "Tsunami on 26 December 2004: Field investigations carried out along the west and south coasts of Sri Lanka". http://www.drs.dpri.kyoto-u.ac.jp/sumatra/srilanka-ut/SriLanka_UTeng.html.

Shibayama, T., Okayasu, A., Wijayaratna, N., Sasaki, J., Suzuki, T. & Jayaratna, R. (2005), "The December 26, 2004 Sumatra Earthquake Tsunami: Field Survey around Southern Part of Sri Lanka". http://www.cvg.ynu.ac.jp/G2/srilanka_survey_ynu_e.html.

The United Kingdom Hydrographic Office. Tidal constituents for the Indian Ocean and South China Sea, *Admiralty Tide Tables*, Vol. 3, The Hydrographic Office, Somerset, UK, 1999.

Tsuji, Y., Namegaya, Y. & Ito, N. (2005), "Astronomical Tide Levels along the Coasts of the Indian Ocean", Earthquake Research Institute, The University of Tokyo. http://www.eri.u-tokyo.ac.jp/ namegaya/ sumatera/ tide/srilanka.htm.

Wijetunge, J. J., Sampath D. M. R., Lubinbert, J. C., Ashok, J., Vakeeswaran, A. & Withanage, P. (2005), "Indian Ocean Tsunami on 26 December 2004: Post-Tsunami Inundation and Run-up Height Survey in Sri Lanka". http://www.civil.pdn.ac.lk/ academic staff/tsunami/tsunami.htm.